

Kent Academic Repository

Full text document (pdf)

Citation for published version

Albasry, Hind and Zhu, Huiling and Wang, Jiangzhou (2018) In-band Emission Interference in D2D-enabled Cellular Networks: Modelling, Analysis, and Mitigation. IEEE Transactions on Wireless Communications . ISSN 1536-1276.

DOI

<https://doi.org/10.1109/TWC.2018.2866833>

Link to record in KAR

<https://kar.kent.ac.uk/69372/>

Document Version

Author's Accepted Manuscript

Copyright & reuse

Content in the Kent Academic Repository is made available for research purposes. Unless otherwise stated all content is protected by copyright and in the absence of an open licence (eg Creative Commons), permissions for further reuse of content should be sought from the publisher, author or other copyright holder.

Versions of research

The version in the Kent Academic Repository may differ from the final published version.

Users are advised to check <http://kar.kent.ac.uk> for the status of the paper. **Users should always cite the published version of record.**

Enquiries

For any further enquiries regarding the licence status of this document, please contact:

researchsupport@kent.ac.uk

If you believe this document infringes copyright then please contact the KAR admin team with the take-down information provided at <http://kar.kent.ac.uk/contact.html>

In-band Emission Interference in D2D-enabled Cellular Network: Modelling, Analysis, and Mitigation

Hind Albasry, Jiangzhou Wang, *Fellow, IEEE*, and Huiling Zhu, *Senior Member, IEEE*

Abstract

Next generation network is considered as a device to device (D2D)-enabled system. The overlay in-band scheme can be used by the cellular user equipments (CUEs) and D2D user equipments (DUEs) to send data. The cellular and D2D links experience the in-band emission interference (IEI) from the DUEs that use the adjacent frequencies. This paper models the IEI impact by using the stochastic geometry and analytically investigates this impact on cellular and D2D links. The IEI inter-cell and IEI intra-cell are separately assessed, and the expected D2D resource block (DRB) reuse factor is evaluated. Further, distance-density based (DDB) strategy is proposed to mitigate the IEI by controlling the number and location of served DUEs for each DRB. Also, optimal power allocation (OPA) algorithm is proposed by calculating the optimal DUEs transmission power profile that mitigates IEI and maximizes the DUEs sum rate. The performance is improved significantly for the proposed methods. The application scenario is identified for each mitigation method.

Index Terms

In-band emission interference, device to device communications, D2D-enabled cellular network, stochastic geometry.

I. INTRODUCTION

DEVICE TO DEVICE (D2D) communication is an integral part of next generation cellular network. D2D supports proximity-based services, reduces end to end latency, extends the cellular coverage, and reduces handset power consumption [4]. D2D communication can also improve the spectral efficiency by reusing the frequency resources within a cell [5]. It is anticipated that the D2D link density in the next generation cellular network will increase

Hind Albasry, Jiangzhou Wang, and Huiling Zhu are with the School of Engineering and Digital Arts, University of Kent, Canterbury, Kent, CT2 7NT, UK (email: {hrja2, j.z.wang, h.zhu}@kent.ac.uk).

The present paper is different from the previous publications in [1]–[3]. This work investigates IEI impact extensively. The propose model is more realistic, the IEI impact is analysed for cellular and also for D2D side. The expected reuse factor is derived. Two novel methods are proposed to mitigate it.

1
2
3
4
5 significantly [6]. Thus, frequency reuse is desirable within the cell in order to use the frequency
6 resources efficiently and cope with high D2D user equipment (DUE) density.
7

8 One of the challenges in D2D-enabled cellular network is in-band emission interference (IEI),
9 which is defined as a power leakage among adjacent frequencies [7]–[12]. In the legacy network,
10 each cellular user equipments (CUEs) uses a dedicated frequency, which causes a negligible
11 leakage power among adjacent frequencies. However, in D2D-enabled cellular network, the
12 frequency resources may be reused by DUEs within the same cell, thanks to the small distance
13 between the transmitter and the receiver of D2D links. However, this causes a non-negligible
14 IEI from DUEs to cellular and D2D links in high dense D2D-enabled cellular network. Thus
15 IEI must be considered, where multiple D2D links reuse the same frequency.
16
17

18 [7]–[11] studied IEI impact in D2D-enabled cellular network and proposed frequency re-
19 sources grouping and different power control schemes to mitigate it. Only simulation system was
20 used to evaluate the IEI impact in these studies. In [7], a D2D frequency resources grouping was
21 proposed, which was motivated by the fact that with DUEs fixed transmit power, the IEI to the
22 base station (BS) mainly comes from the cell centre DUEs. However, the proposed frequency
23 resources grouping method mitigated the IEI for just cell edge frequency resources group, where
24 the impact still exists in centre edge frequency resources group. Further, [8]–[12] proposed a
25 power control methods to mitigate IEI. [8] proposed BS based open loop power control (OLPC)
26 algorithm for D2D, where the IEI from DUEs to cellular links was controlled by the BS. In
27 [9], the proposed scheme controlled the DUEs transmission power according to the DUEs
28 locations from the serving BS by utilizing the distance-proportional fractional power control.
29 The proposed methods in [9] and [8] are OLPC methods and impose constraints on the DUEs
30 transmission power, which affects the performance of DUEs. Thus, [10]–[12] proposed strategies
31 to relax the power constraints of OLPC methods, where the DUEs can increase the transmission
32 power. The main idea is identify additional slots, where the DUEs can boost the transmission
33 power without affecting the cellular links. However, in the proposed OLPC-based methods, the
34 DEUs transmission power is constrained without taking into account that can affect the DUEs
35 performance.
36
37
38
39
40
41
42
43
44
45
46
47
48
49
50
51

52 Since the D2D communication is one of the main parts of future networks and the IEI is
53 expected to be a serious problem, this gives us a motivation to propose a new framework model to
54 evaluate theoretically the D2D-enabled cellular network by considering the IEI impact. Further,
55
56
57
58
59
60

the mitigation methods proposed by the literature did not give much attention to D2D links performance. Therefore, in this paper, two mitigation methods are proposed: frequency resources grouping strategy and power control algorithm that take into account performance of D2D and cellular links in the network. The paper contributions can be summarized as follows:

- 1) A framework system model is proposed by using a stochastic geometry, which considers the IEI impact for high dense D2D-enabled cellular network. The IEI impact is evaluated for the cellular and D2D links. A closed-form of CUE coverage probability and data rate are derived to evaluate the cellular link performance, and DUE successful probability and data rate are derived to evaluate the D2D link performance. Further, the D2D resource blocks (DRBs) expected reuse factor is derived, which satisfies the quality of service (QoS) requirements of the cellular and D2D links.
- 2) The evaluation results show that the IEI is more severe on cellular than D2D links. Thus, this work proposes a frequency resources grouping and the power allocation strategies to mitigate the IEI on cellular links. The application scenario of each mitigation method is explained and compared with the literature schemes. Both methods take into account the cellular and D2D links performance.
 - A frequency resources grouping method called distance-density based (DDB) strategy is proposed to mitigate the IEI. Based on the fact that the nearest DRBs to the cellular resource blocks (CRBs) cause more IEI, a protection band is defined. The number and the locations of DUEs in this band is controlled by the BS within one cell and modelled using thinning process and Poisson hole process (PHP). The optimal protection band size for each cell is found which maximizes the cellular link coverage probability. The system performance is evaluated and the results show the significant improvement is achieved by employing this strategy.
 - The impact of IEI intra-cell (IEI from the same cell) and inter-cell (IEI from other cells) on cellular link are investigated. The results show that the IEI intra-cell dominates the IEI inter-cell when the DUE density is high. Thus, we propose optimal power allocation (OPA) algorithm to eliminate the IEI intra-cell within one cell. The problem is formulated as an optimization problem that maximizes the DUEs sum rate under constraint that the leakage from each DRBs does not exceed the interference threshold at the BS. The cellular link coverage probability is improved significantly by employing this algorithm.

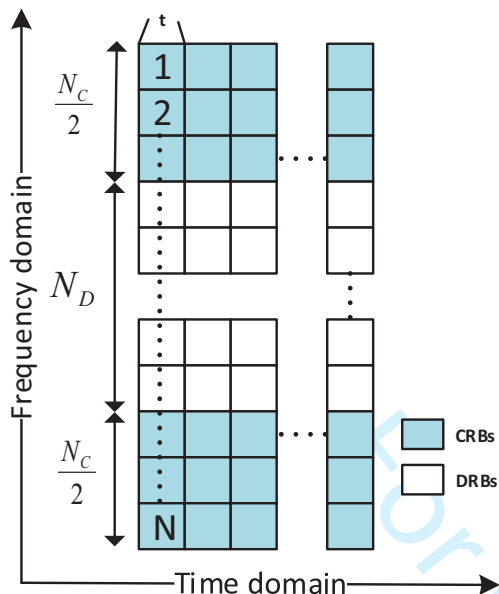


Fig. 1: Overlay frequency resources model.

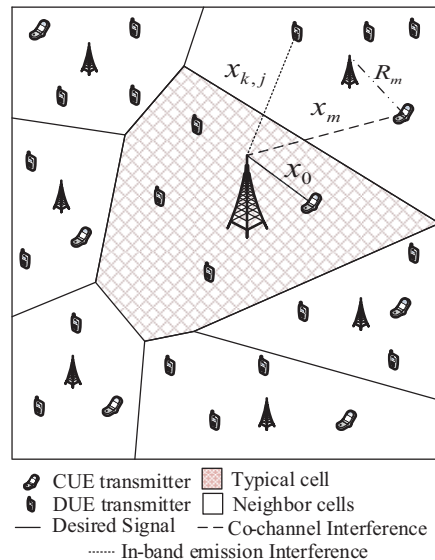


Fig. 2: Network Model.

The remainder of the paper is organized as follows. In Section II, the system model of D2D-enabled cellular network is described. In Section III, the network performance is analysed. In Section IV, two methods are proposed to mitigate the IEI impact. The results and the discussion are provided in Section V. The conclusion is followed in Section VI.

II. SYSTEM MODEL

Consider the IEI impact for D2D overlay in-band scheme, using the uplink frequency resources pool structure proposed by 3rd generation partnership project (3GPP) [10], [11], as shown in Fig. 1. The CUEs use CRBs to transmit the uplink traffic, while DUEs use DRBs to transmit D2D data. N_C and N_D represent the numbers of CRBs and DRBs in each time slot t , where $N_C + N_D = N$ and N is the total number of resource blocks (RBs) in t . For network model, consider D2D-enabled orthogonal frequency division multiple access (OFDMA)-based cellular network with multiple cells [13]–[15], as shown in Fig. 2. The locations of BSs, the CUEs using the i th CRB, and the DUEs using the j th DRBs are modelled as independent homogeneous Poisson point processes (PPPs) Φ , Φ_i , and Φ_j with densities of λ , λ_i and λ_j respectively, where

$$i \in \{1, 2, \dots, N_C\} \quad \text{and} \quad j \in \{1, 2, \dots, N_D\}.$$

A full load scenario is assumed, where each CRB is occupied by one CUE in each cell, thus λ_i and λ have equal values. Further, each DRB can be reused by r_d DUEs, where r_d is the reuse

factor of DRBs for each cell in the network. Also, it is assumed that each DUE uses only one DRB to transmit D2D data.

In this model, the signals experience distance dependent path loss with a path loss exponent α , and fast fading. The fast fading power gain follows the exponential distribution with mean $\frac{1}{\mu}$, which it is denoted by $h \sim \exp(\mu)$. One RB subcarriers are characterised by the same channel gain. A fractional path loss-inversion based power control is considered of form $x^{\alpha\epsilon}$, where x represents the distance, and $\epsilon \in [0, 1]$ is the power control factor. The distances are assumed independent and identically distributed (i.i.d) and follow Rayleigh distribution [5]. Further, IEI from a DUE using the j th DRB to a CUE using the i th CRB can be expressed in the form of

$$IeI_i = P_D h_{k,j} x_{k,j}^{-\alpha} \xi_{j,i},$$

where P_D is the DUE transmission power, $h_{k,j}$ and $x_{k,j}^{-\alpha}$ denote the channel gain and path loss between IEI interferer DUE k th and the BS, and $\xi_{j,i}$ is the ratio of the power measured at the j th DRB to the power measured at the i th CRB [16].

Since each CRB is occupied by one CUE and the DRBs can be reused by r_d within one cell, thus the density of CUEs use i th CRB is significantly lower than the DUEs's use j th DRB. Therefore, the leakage power among the CUEs is dominated by the IEI from the DUEs and can be neglected and also the leakage from the CUEs to the DUEs.

Following the above assumptions, we define the typical CUE as the closest uplink user to the serving BS that uses i th CRB to transmit data in the typical cell, where the BS is centred at the origin as a reference, see Fig. 2. The uplink signal to interference and noise ratio (SINR) of the typical CUE at the BS can be expressed as

$$SINR_i = \frac{P_C h_0 x_0^{\alpha(\epsilon-1)}}{I_i + IEI_i + \sigma^2}, \quad (1)$$

where P_C represents CUE constant baseline transmission power. 0 denotes the typical CUE that uses i th CRB. h_0 denotes the distance-independent channel gain between the typical CUE and the reference BS. x_0 is the distance between the typical CUE and the reference BS. I_i denotes the cumulative co-channel interference from interferer CUEs at the reference BS. IEI_i is cumulative IEI from interferer DUEs at the reference BS. σ^2 is noise power. I_i is given by

$$I_i = \sum_{m \in \Phi_i/0} P_C R_m^{\alpha\epsilon} h_m x_m^{-\alpha},$$

where m denotes co-channel interferer CUE to typical CUE. R_m is the distance between the co-channel interferer CUE and its serving BS. h_m denotes the distance-independent channel gain

between the co-channel interferer CUE and the reference BS. x_m is the distance between the co-channel interferer CUE and the reference BS. IEI_i is expressed by

$$IEI_i = \sum_{j=1}^{N_D} \sum_{k \in \Phi_j} I_e I_i = \sum_{j=1}^{N_D} \sum_{k \in \Phi_j} P_D h_{k,j} x_{k,j}^{-\alpha} \xi_{j,i},$$

where k denotes IEI interferer DUE to typical CUE. $h_{k,j}$ denotes the distance-independent channel gain between the IEI interferer DUE and the reference BS. $x_{k,j}$ is the distance between the IEI interferer DUE and the reference BS.

Furthermore, we define a typical D2D pair, where a typical DUE transmitter locates far from the reference DUE receiver by distance x_{d_0} , and find the typical DUE SINR as

$$SINR_{j_0} = \frac{P_D h_{d_0} x_{d_0}^{-\alpha}}{I_{j_0} + IEI_{j_0} + \sigma^2}, \quad (2)$$

where $j_0 \in \{1, 2, \dots, N_D\}$. d_0 is typical DUE that uses j_0 th DRB. h_{d_0} denotes the distance-independent channel gain between the typical DUE and the reference DUE receiver. x_{d_0} is the distance between the typical DUE and the reference DUE receiver. I_{j_0} denotes the cumulative co-channel interference from the interferer DUEs at the reference DUE receiver. IEI_{j_0} is the cumulative IEI from the interferer DUEs at the reference DUE receiver. I_{j_0} is given by

$$I_{j_0} = \sum_{d_m \in \Phi_j/d_0} P_D h_{d_m} x_{d_m}^{-\alpha},$$

where d_m is co-channel interferer DUE to typical DUE. h_{d_m} denotes the distance-independent channel gain between the co-channel interferer DUE and the reference DUE receiver. x_{d_m} is the distance between the co-channel interferer DUE and the reference DUE receiver. IEI_{j_0} is expressed by

$$IEI_{j_0} = \sum_{j=1}^{N_D} \sum_{d \in \Phi_j} P_D h_{d,j} x_{d,j}^{-\alpha} \xi_{j,j_0},$$

where d denotes IEI interferer DUE to typical DUE. h_{d,j_0} denotes the distance-independent channel gain between the IEI interferer DUE and the reference DUE receiver. x_{d,j_0} is the distance between the IEI interferer DUE and the reference DUE receiver. ξ_{j,j_0} represents the ratio of the power measured at the j th DRB to the power measured at the j_0 th DRB.

III. PERFORMANCE ANALYSIS

In this section, we analyse the performance of the cellular and D2D links in D2D-enabled cellular network by taking into account the IEI impact. The IEI intra-cell and IEI inter-cell are analysed separately under the main framework. Finally, the optimal expected DRB reuse factor is calculated within one cell, which maximizes the cellular link coverage probability and satisfies

the given QoS constrains for cellular and D2D links. The analysis in this paper is for one time slot, which can be generalized to all time slots.

A. Cellular Link

The cellular link coverage probability in D2D-enabled cellular network is defined as the probability that the uplink SINR of the CUE at its serving BS is greater than the SINR threshold β , which is given by

$$P_{cov_i} = \mathbb{E}_{x_0} \left[\mathbb{P}(SINR_i \geq \beta \mid x_0) \right]. \quad (3)$$

P_{cov_i} is averaged over the plane conditioned on the closest CUE (typical CUE) being at the distance x_0 . It is assumed that x_0 follows a Rayleigh distribution and the probability density function (PDF) is found from null probability of a 2-D Poisson process [17] as

$$f(x_0) = 2\pi\lambda_i x_0 e^{-\pi\lambda_i x_0^2}. \quad (4)$$

Thus, the coverage probability in (3) can be rewritten as

$$\begin{aligned} P_{cov_i} &= \int_0^\infty \mathbb{P}[SINR_i \geq \beta \mid x_0] \cdot f(x_0) dx_0 \\ &= \int_0^\infty \mathbb{P}[h_0 \geq \beta P_C^{-1} x_0^{\alpha(1-\epsilon)} (I_i + IEI_i + \sigma^2) \mid x_0] \cdot 2\pi\lambda_i x_0 e^{-\pi\lambda_i x_0^2} dx_0. \end{aligned} \quad (5)$$

The conditional coverage probability in (5) can be denoted by $p_i(x_0)$ and derived as

$$p_i(x_0) = \mathbb{P}[h_0 \geq \beta P_C^{-1} x_0^{\alpha(1-\epsilon)} (I_i + IEI_i + \sigma^2) \mid x_0] \stackrel{(a)}{=} \mathcal{L}_{I_i}(s) \cdot \mathcal{L}_{IEI_i}(s) \cdot \exp(-s\sigma^2), \quad (6)$$

where (a) follows the fact that $h_0 \sim \exp(\mu)$, the definition of interference Laplace transform $\mathcal{L}_I(s) = \mathbb{E}_I[\exp(-sI)]$ [18], and by letting $s = \beta\mu P_C^{-1} x_0^{\alpha(1-\epsilon)}$.

$\mathcal{L}_{I_i}(s)$ and $\mathcal{L}_{IEI_i}(s)$ are defined as follows. $\mathcal{L}_{I_i}(s)$ is Laplace transform of the cumulative co-channel interference of the CUEs at the reference BS given by

$$\mathcal{L}_{I_i}(s) = \exp(-\pi\lambda_i \varrho(s)), \quad (7)$$

where

$$\varrho(s) = \varrho(\beta, x_0, \epsilon, \alpha) = \left(\frac{\mu}{s P_C \mathbb{E}_{R_m} [R_m^{\alpha\epsilon}]} \right)^{-\frac{2}{\alpha}} \int_{u(x_0)}^\infty \frac{1}{1+u^{\frac{\alpha}{2}}} du, \quad (8)$$

and

$$u(x_0) = \left(\frac{\mu}{s P_C \mathbb{E}_{R_m} [R_m^{\alpha\epsilon}]} \right)^{\frac{2}{\alpha}} x_0^2.$$

proof: see Appendix A.

Furthermore, $\mathcal{L}_{IEI_i}(s)$ is the Laplace transform of cumulative IEI of the DUEs at the reference BS given by

$$\mathcal{L}_{IEI_i}(s) = \exp\left(-\frac{2\pi^2}{\sin \frac{2\pi}{\alpha}} \lambda_j \left(\frac{\mu}{s P_D} \right)^{-\frac{2}{\alpha}} \sum_{j=1}^{N_D} \left[\xi_{j,i}^{\frac{2}{\alpha}} \right] \right). \quad (9)$$

proof: see Appendix B.

Now we derive the coverage probability of typical CUE by substituting (7) and (9) in (6) and then (6) in (5), and by plugging $s = \beta\mu P_C^{-1}x_0^{\alpha(1-\epsilon)}$, we get

$$P_{cov_i} = \int_0^\infty 2\pi\lambda_i x_0 e^{-\pi\lambda_i x_0^2} \cdot \exp(-\pi\lambda_i \varrho(\beta, x_0, \epsilon, \alpha)) \cdot \exp(-\psi(\beta)x_0^{2(1-\epsilon)}) \cdot \exp(-\beta\mu P_C^{-1}x_0^{\alpha(1-\epsilon)}\sigma^2) dx_0, \quad (10)$$

where

$$\psi(\beta) = \frac{2\pi^2}{\sin \frac{2\pi}{\alpha}} \lambda_j \beta^{\frac{2}{\alpha}} \left(\frac{P_D}{P_C}\right)^{\frac{2}{\alpha}} \sum_{j=1}^{N_D} \left[\xi_{j,i}^{\frac{2}{\alpha}}\right].$$

Special case: To shed further light on the significance of the expression in (10), the coverage probability is calculated for interference-limited regime $\sigma^2 = 0$, with power control factor $\epsilon = 0$, which is reduced to

$$P_{cov_i} = \int_0^\infty 2\pi\lambda_i x_0 e^{-(\pi\lambda_i + \pi\lambda_i \bar{\varrho}(\beta, \epsilon=0, \alpha) + \psi(\beta))x_0^2} dx_0, \quad (11)$$

where $\varrho(\beta, x_0, \epsilon, \alpha)$ in (10) is substituted by

$$\varrho(\beta, x_0, \epsilon, \alpha) = \bar{\varrho}(\beta, \epsilon = 0, \alpha) x_0^2.$$

From (8), we can derive $\bar{\varrho}(\beta, \epsilon = 0, \alpha)$ as

$$\bar{\varrho}(\beta, \epsilon = 0, \alpha) = \beta^{\frac{2}{\alpha}} \int_{\beta^{-\frac{2}{\alpha}}}^\infty \frac{1}{1+u^{\frac{\alpha}{2}}} du. \quad (12)$$

The coverage probability special case closed-form is given as

$$P_{cov_i} = \frac{1}{1 + \beta^{\frac{2}{\alpha}} \int_{\beta^{-\frac{2}{\alpha}}}^\infty \frac{1}{1+u^{\frac{\alpha}{2}}} du + \frac{\psi(\beta)}{\pi\lambda_i}}. \quad (13)$$

Note that the IEI impact changes according to the location of CRB [8]. Thereby, the expected value of the coverage probability over the given CRBs can be calculated as

$$\bar{P}_{cov} = \sum_{i=1}^{N_c} P_{cov_i} P_r, \quad (14)$$

where P_r is the probability of the i th CRB assigned to the typical CUE and given by $P_r = \frac{1}{N_c}$, as the CRBs can be allocated to any CUE in the network.

On the other hand, the expected data rate can be defined as

$$R_C = \mathbb{E}[\ln(1 + SINR_i)] \stackrel{(a)}{=} \int_0^\infty \mathbb{P}[SINR_i > (e^{\mathfrak{S}} - 1)] d\mathfrak{S}, \quad (15)$$

where (a) follows because $\ln(1 + SINR_i)$ is strictly positive variable. Letting $\chi = (e^{\mathfrak{S}} - 1)$ and using the SINR distribution of typical CUE given in (13), we get

$$R_C = \int_0^\infty \mathbb{P}[SINR_i \geq \chi] \frac{d\chi}{\chi + 1} = \int_0^\infty \frac{P_{cov_i}(\chi)}{\chi + 1} d\chi. \quad (16)$$

$P_{cov_i}(\chi)$ can be obtained by generalizing P_{cov_i} given by (13), and replacing β by χ . Thereby, the expected data rate can be obtained by plugging $P_{cov_i}(\chi)$ in (16) as

$$R_C = \int_0^\infty \frac{1}{(\chi + 1) \left(1 + \chi^{\frac{2}{\alpha}} \int_{\chi^{-\frac{2}{\alpha}}}^\infty \frac{1}{1+u^{\frac{\alpha}{2}}} du + \frac{\psi(\chi)}{\pi\lambda_i} \right)} d\chi. \quad (17)$$

To solve (17), we need to defined the path loss exponent. Consider the lossy environment, where $\alpha = 4$, the expected data rate can be given by

$$R_C = \int_0^\infty \frac{1}{(\chi + 1) \left(1 + \chi^{\frac{1}{2}} \left[\frac{\pi}{2} - \tan^{-1} \left(\chi^{-\frac{1}{2}} \right) \right] + \frac{\psi(\chi)}{\pi\lambda_i} \right)} d\chi, \quad (18)$$

which can be easily calculated numerically.

B. D2D Link

The successful probability of D2D link is defined as a probability that the D2D pair can establish a link to transmit data, and the SINR at the receiver is greater than the SINR threshold β_d . The successful probability for the typical DUE transmitter located at distance x_{d_0} from the reference DUE receiver is given by

$$\begin{aligned} P_{suc_{j_0}} &= \mathbb{P}(SINR_{j_0} \geq \beta_d) = \mathbb{P}[h_{d_0} \geq \beta_d P_D^{-1} x_{d_0}^\alpha (I_{j_0} + IEI_{j_0} + \sigma^2)] \\ &= \mathcal{L}_{I_{j_0}}(s_d) \cdot \mathcal{L}_{IEI_{j_0}}(s_d) \cdot \exp(-s_d \sigma^2), \end{aligned} \quad (19)$$

where $s_d = \beta_d \mu P_D^{-1} x_{d_0}^\alpha$. $\mathcal{L}_{I_{j_0}}(s_d)$ is Laplace transform of the cumulative co-channel interference of the DUEs at the reference DUE receiver, which is derived as Appendix A

$$\mathcal{L}_{I_{j_0}}(s_d) = \exp\left(-\frac{2\pi^2}{\alpha} \lambda_j \left(\frac{\mu}{s_d P_D}\right)^{-\frac{2}{\alpha}}\right). \quad (20)$$

However, in this case, Φ_j probability generating functional (PGFL) function integration limits for the DUEs are from 0 to ∞ since the closest co-channel interferer could be very close to the reference DUE receiver. $\mathcal{L}_{IEI_{j_0}}(s_d)$ is Laplace transform of cumulative IEI of the DUEs at the reference DUE receiver, which is derived similarly to Appendix B, and given by

$$\mathcal{L}_{IEI_{j_0}}(s_d) = \exp\left(-\frac{2\pi^2}{\alpha} \lambda_j \left(\frac{\mu}{s_d P_D}\right)^{-\frac{2}{\alpha}} \sum_{j=1}^{N_D} \left[\xi_{j,j_0}^{\frac{2}{\alpha}}\right]\right). \quad (21)$$

For interference limited regime, the successful probability of typical DUE is obtained by substituting (20) and (21), and plugging $s_d = \beta_d \mu P_D^{-1} x_{d_0}^\alpha$ in (19) as

$$P_{suc_{j_0}} = \exp\left(-\psi_d(\beta_d) x_{d_0}^2 \left(1 + \sum_{j=1}^{N_D} \left[\xi_{j,j_0}^{\frac{2}{\alpha}}\right]\right)\right), \quad (22)$$

where

$$\psi_d(\beta_d) = \frac{2\pi^2}{\alpha} \lambda_j \beta_d^{\frac{2}{\alpha}}.$$

The expected value of successful probability over the given DRBs can be calculated as

$$\bar{P}_{suc} = \sum_{j=1}^{N_D} P_{sucj} P_{rd}, \quad (23)$$

where P_{rd} is the probability of the j th DRB assigned to the typical DUE and given by $P_{rd} = \frac{1}{N_D}$, as the DRBs can be allocated to any DUE in the network.

The expected data rate of the typical DUE link can be defined as

$$R_D = \int_0^\infty \mathbb{P}[SINR_{j_0} \geq \chi_d] \frac{d\chi_d}{\chi_d + 1} = \int_0^\infty \frac{P_{sucj_0}(\chi_d)}{\chi_d + 1} d\chi_d. \quad (24)$$

$P_{sucj_0}(\chi_d)$ can be obtained by generalizing P_{sucj_0} given by (22), and replacing β_d by χ_d . Thereby, the data rate can be derived by plugging $P_{sucj_0}(\chi_d)$ in (24) as

$$R_D = \int_0^\infty \frac{\exp\left(-\psi_d(\chi_d) x_{d_0}^2 \left(1 + \sum_{j=1}^{N_D} \left[\xi_{j,j_0}^{\frac{2}{\alpha}}\right]\right)\right)}{(\chi_d + 1)} d\chi_d, \quad (25)$$

which also can be easily calculated numerically.

C. IEI inter-cell and IEI intra-cell

The IEI may have big impact on system performance, in this subsection, we study which IEI dominates the cellular link performance in each cell IEI intra-cell or IEI inter-cell, which are defined as the IEI within the typical cell and the IEI from other cells, respectively. The Laplace transform of the cumulative IEI of the DUEs at the reference BS $\mathcal{L}_{IEI_i}(s)$ can be expressed in terms of Laplace transform of IEI intra-cell and IEI inter-cell and rewritten as

$$\mathcal{L}_{IEI_i}(s) = \mathcal{L}^{(O)}_{IEI_i}(s) \cdot \mathcal{L}^{(\hat{O})}_{IEI_i}(s), \quad (26)$$

where $\mathcal{L}^{(O)}_{IEI_i}(s)$ represents the Laplace transform of cumulative IEI of the DUEs at the reference BS within the typical cell, and $\mathcal{L}^{(\hat{O})}_{IEI_i}(s)$ represents the Laplace transform of the cumulative IEI of the DUEs at the reference BS from other cells. By following the derivation in Appendix B, we get $\mathcal{L}^{(O)}_{IEI_i}(s)$ and $\mathcal{L}^{(\hat{O})}_{IEI_i}(s)$ as

$$\mathcal{L}^{(O)}_{IEI_i}(s) = \exp\left(-2\pi\lambda_j \left(\frac{\mu}{sP_D}\right)^{-\frac{2}{\alpha}} \sum_{j=1}^{N_D} \left[\xi_{j,i}^{\frac{2}{\alpha}}\right] \int_0^{\mathfrak{R}} \frac{v}{1+v^\alpha} dv\right), \quad (27)$$

and

$$\mathcal{L}^{(\hat{O})}_{IEI_i}(s) = \exp\left(-2\pi\lambda_j \left(\frac{\mu}{sP_D}\right)^{-\frac{2}{\alpha}} \sum_{j=1}^{N_D} \left[\xi_{j,i}^{\frac{2}{\alpha}}\right] \int_{\mathfrak{R}}^\infty \frac{v}{1+v^\alpha} dv\right), \quad (28)$$

where integration limits of Φ_j PGFL function are taken from 0 to \mathfrak{R} for IEI intra-cell, and from \mathfrak{R} to ∞ for IEI inter-cell, where \mathfrak{R} is the typical cell radius. The coverage probability in terms of the IEI intra-cell and IEI inter-cell can be obtained by substituting (7) and (26), and plugging $s = \beta\mu P_C^{-1} x^{\alpha(1-\epsilon)}$ in (6) and then in (5) as

$$P_{cov_i} = \int_0^\infty 2\pi\lambda_i x_0 e^{-\pi\lambda_i x_0^2} \cdot \exp\left(-\pi\lambda_i \hat{\delta}(\beta, x_0, \epsilon)\right) \cdot \exp(-\varpi x_0^{2(1-\epsilon)}) \cdot \exp(-\varsigma x_0^{2(1-\epsilon)}) \cdot \exp(-\beta\mu P_C^{-1} x_0^{\alpha(1-\epsilon)} \sigma^2) dx_0, \quad (29)$$

where ϖ and ς are the IEI intra-cell and IEI inter-cell terms given by

$$\varpi = 2\pi\lambda_j \beta^{\frac{2}{\alpha}} \left(\frac{P_D}{P_C}\right)^{\frac{2}{\alpha}} \sum_{j=1}^{N_D} \left[\xi_{j,i}^{\frac{2}{\alpha}}\right] \left(\int_0^{\mathfrak{R}} \frac{v}{1+v^\alpha} dv\right),$$

and

$$\varsigma = 2\pi\lambda_j \beta^{\frac{2}{\alpha}} \left(\frac{P_D}{P_C}\right)^{\frac{2}{\alpha}} \sum_{j=1}^{N_D} \left[\xi_{j,i}^{\frac{2}{\alpha}}\right] \left(\int_{\mathfrak{R}}^\infty \frac{v}{1+v^\alpha} dv\right).$$

By considering the special case ($\sigma^2 = 0, \epsilon = 0$) as (13), we obtain the coverage probability in terms of IEI intra-cell and IEI inter-cell as

$$P_{cov_i} = \frac{1}{1 + \beta^{\frac{2}{\alpha}} \int_{\beta^{-\frac{2}{\alpha}}}^\infty \frac{1}{1+u^{\frac{\alpha}{2}}} du + \frac{\varpi+\varsigma}{\pi\lambda_i}}. \quad (30)$$

D. Expected DRB reuse factor

In this subsection, we derive the optimal expected reuse factor of DRBs for each cell in terms of QoS parameters. The reuse factor can be defined as the number of DUEs can reuse each DRB within one cell. λ_j in (13) and (22) can be expressed in terms of r_d as

$$\lambda_j = \frac{r_d}{\pi\mathfrak{R}^2} = \frac{16r_d\lambda}{\pi}, \quad (31)$$

where \mathfrak{R} is the expected cell radius in the random networks, which is given by

$$\mathfrak{R} = \frac{1}{4\sqrt{\lambda}}. \quad (32)$$

CUE coverage probability threshold P_{cov}^{th} and DUE successful probability threshold P_{suc}^{th} are defined as QoS thresholds for CUEs and DUEs that guarantee reuse of DRBs without causing a harmful interference to cellular and D2D links.

For comparison sake, we consider IEI and no IEI case. In case the IEI is taken into account, the reuse of DRB affects both cellular link coverage probability and D2D link successful probability, adversely. Thus, we derive optimal r_d that maximizes the coverage probability and the successful probability in (13) and (22), and fulfills the QoS thresholds requirements as follows

$$\text{minimize } r_d \quad (33)$$

$$\text{subject to } \frac{1}{1 + \beta^{\frac{2}{\alpha}} \int_{\beta^{-\frac{2}{\alpha}}}^\infty \frac{1}{1+u^{\frac{\alpha}{2}}} du + \hat{\psi}r_d} \geq P_{cov}^{th} \quad (33a)$$

$$\exp\left(-\hat{\psi}r_d\right) \geq P_{suc}^{th}, \quad (33b)$$

where

$$\hat{\psi} = \frac{32}{\alpha} \beta^{\frac{2}{\alpha}} \left(\frac{P_D}{P_C} \right)^{\frac{2}{\alpha}} \sum_{j=1}^{N_D} \left[\xi_{j,i}^{\frac{2}{\alpha}} \right],$$

and

$$\hat{\psi}_d = \frac{32\pi}{\alpha} \lambda \beta_d^{\frac{2}{\alpha}} x_{d_0}^2 \left(1 + \sum_{j=1}^{N_D} \left[\xi_{j,j_0}^{\frac{2}{\alpha}} \right] \right).$$

From (33a) and (33b), we can find optimal expected reuse factor for IEI case as

$$r_d^* = \min \left\{ \frac{(P_{cov}^{th})^{-1} - \beta^{\frac{2}{\alpha}} \int_{\beta^{-\frac{2}{\alpha}}}^{\infty} \frac{1}{1+u^{\frac{\alpha}{2}}} du - 1}{\hat{\psi}}, \frac{-\ln(P_{suc}^{th})}{\hat{\psi}_d} \right\}. \quad (34)$$

For no IEI case, the IEI is not taken into account, the reuse of DRBs affects only the D2D link successful probability, adversely. Thus, we find the optimal reuse factor that maximizes the DUE successful probability in (22), where the DUEs can reuse the DRB on condition that the DUEs successful probability satisfies the threshold given by $P_{suc}^{th-no IEI}$. Since, the DUEs do not experience the IEI, we let $\xi_{j,j_0} = 0$ in (22) and derive the $r_{d-no IEI}$ that satisfies the required $P_{suc}^{th-no IEI}$ as

$$\text{minimize } r_{d-no IEI} \quad (35)$$

$$\text{subject to } \exp(-\tilde{\psi}_d r_{d-no IEI}) \geq P_{suc}^{th-no IEI}, \quad (35a)$$

where

$$\tilde{\psi}_d = \frac{32\pi}{\alpha} \lambda \beta_d^{\frac{2}{\alpha}} x_{d_0}^2. \quad (36)$$

The optimal expected reuse factor for no IEI case is derived as

$$r_{d-no IEI}^* = \frac{-\ln(P_{suc}^{th-no IEI})}{\tilde{\psi}_d}. \quad (37)$$

IV. IEI MITIGATION

From subsection A in the results section, the IEI impact on the cellular links is more severe than the D2D links. Thus, this work focuses on the IEI impact on cellular link and propose methods to mitigate this effect. Henceforth, the IEI denotes the IEI impact on the cellular link. The main parameters that can control the IEI are DUE density, DUEs locations, and DUEs transmission power. Hence, we propose two mitigation methods: the DDB strategy and the OPA algorithm. The formal one controls DUE density and DUEs locations that use the adjacent DRBs to the CRBs and the second method controls the DUEs transmission power.

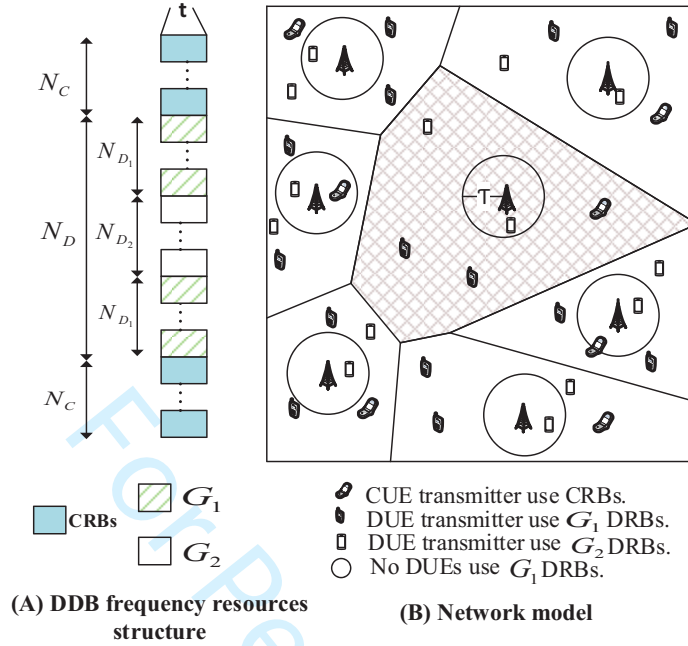


Fig. 3: DDB strategy.

A. Distance-density based (DDB) strategy

Based on the fact that the nearest DRBs cause more IEI [8], it is expected that the IEI can be mitigated if the number of DUEs use the DRBs located next to the CRBs is controlled and also if these DUEs are located far from the serving BS. Accordingly, we define the protection band, where the number and location of DUEs that use the DRBs in this band are controlled by the BS. In this section, we remodel and re-analyse the system, and evaluate the network performance in terms of the new DRBs groups setting. Then, we find the optimal DRBs groups setting, which maximizes the cellular link coverage probability and guarantees serving the required number of DUEs within one cell.

Fig. 3-A shows the DDB frequency resources structure in each t , where G_1 and G_2 denote the protection and typical bands DRBs, respectively. N_{D_1} and N_{D_2} represent the number of DRBs in G_1 and G_2 , where $N_D = N_{D_1} + N_{D_2}$, and

$$j_1 \in \{1, 2, \dots, N_{D_1}\} \quad \text{and} \quad j_2 \in \{1, 2, \dots, N_{D_2}\}.$$

In typical band, the DUEs locations are modelled as PPP Φ_j with density λ_j . Meanwhile, in protection band, the DUE density and DUEs locations are modelled in terms of reduction factor ρ (to control DUE density) and exclusion distance τ (to control DUEs locations from the serving BS), where ρ is the density control parameter and τ is the radius of the exclusion area, in which

the G_1 DRBs are only assigned to the DUEs located beyond this distance in each cell.

To remodel the DUEs that use the protection band DRBs in the network, we use random thinning operation and PHP [18]. By thinning, the DUEs of Φ_j process are retained with probability ρ to form a new point process $\bar{\Phi}_j$ with density $\rho\lambda_j$, where ρ can take value in the range $[0,1]$. Thus, we can control the DUE density of the DUEs that use G_1 DRBs. Further, we model the DUEs locations in G_1 that locate beyond the exclusion distance τ in terms of $\bar{\Phi}_j$ by using a PHP as shown in Fig. 3-B. The PHP is defined in terms of two independent homogeneous PPPs $\bar{\Phi}_j$ and Φ , where $\bar{\Phi}_j$ represents a PPP from which the holes are carved out and Φ represents the locations of the holes (BSs), which are centered by the BSs and have τ radius. The result process is $\hat{\Phi}_j$ with density $\rho\lambda_j e^{-\pi\lambda\tau^2}$. By PHP, we allocate the G_1 DRBs to the DUEs that only located beyond distance τ from the BS. Accordingly, we have two different processes: $\hat{\Phi}_j$ with density $\rho\lambda_j e^{-\pi\lambda\tau^2}$ for the DUEs use G_1 DRBs, and Φ_j with density λ_j for the DUEs use G_2 DRBs.

For simplicity, we denote this strategy as (\hat{s}) in the derivation. The conditional coverage probability in (6) for this case can be given by

$$p_i^{(\hat{s})} = \mathcal{L}_{I_i}(s) \cdot \mathcal{L}_{IEI_{G_1,i}}^{(\hat{s})}(s) \cdot \mathcal{L}_{IEI_{G_2,i}}^{(\hat{s})}(s) \cdot \exp(-s\sigma^2), \quad (38)$$

where $\mathcal{L}_{IEI_{G_1,i}}^{(\hat{s})}(s)$ and $\mathcal{L}_{IEI_{G_2,i}}^{(\hat{s})}(s)$ are the Laplace transform of cumulative IEI of the DUEs that use G_1 DRBs and G_2 DRBs, respectively, which are given by

$$\mathcal{L}_{IEI_{G_1,i}}^{(\hat{s})}(s) = \exp\left(-\rho e^{-\pi\lambda\tau^2} \psi_1(\beta) x_0^{2(1-\epsilon)}\right),$$

and

$$\mathcal{L}_{IEI_{G_2,i}}^{(\hat{s})}(s) = \exp\left(-\psi_2(\beta) x_0^{2(1-\epsilon)}\right),$$

where

$$\psi_1(\beta) = \frac{2\pi^2}{\sin \frac{2\pi}{\alpha}} \lambda_j \beta^{\frac{2}{\alpha}} \left(\frac{P_D}{P_C}\right)^{\frac{2}{\alpha}} \sum_{j_1=1}^{N_{D_1}} \xi_{j_1,i}^{\frac{2}{\alpha}}, \quad (39)$$

and

$$\psi_2(\beta) = \frac{2\pi^2}{\sin \frac{2\pi}{\alpha}} \lambda_j \beta^{\frac{2}{\alpha}} \left(\frac{P_D}{P_C}\right)^{\frac{2}{\alpha}} \sum_{j_2=1}^{N_{D_2}} \xi_{j_2,i}^{\frac{2}{\alpha}}. \quad (40)$$

The CUE coverage probability for the proposed strategy is obtained as

$$P_{cov_i}^{(\hat{s})} = \int_0^\infty 2\pi\lambda_i x_0 e^{-\pi\lambda_i x_0^2} \cdot \exp(-\pi\lambda_i \varrho(\beta, x_0, \epsilon)) \cdot \exp\left(-\rho e^{-\pi\lambda\tau^2} \psi_1(\beta) x_0^{2(1-\epsilon)}\right) \cdot \exp\left(-\psi_2(\beta) x_0^{2(1-\epsilon)}\right) \cdot \exp\left(-\beta\mu P_C^{-1} x_0^{\alpha(1-\epsilon)} \sigma^2\right) dx_0. \quad (41)$$

The closed-form expression of CUE coverage probability at i th CRB is derived under the proposed strategy, where $\epsilon = 0$ and $\sigma^2 = 0$ as follows

$$P_{cov_i}^{(\hat{s})} = \frac{1}{1 + \beta^{\frac{2}{\alpha}} \int_{\beta^{-\frac{2}{\alpha}}}^{\infty} \frac{1}{1+u^{\frac{\alpha}{2}}} du + \frac{\rho e^{-\pi\lambda\tau^2} \psi_1(\beta) + \psi_2(\beta)}{\pi\lambda_i}}. \quad (42)$$

Also, the expected data rate for this strategy can be derived and given by

$$R_C^{(\hat{s})} = \int_0^{\infty} \frac{P_{cov_i}^{(\hat{s})}(\chi)}{\chi + 1} d\chi = \int_0^{\infty} \frac{1}{(\chi + 1) \left(1 + \beta^{\frac{2}{\alpha}} \int_{\beta^{-\frac{2}{\alpha}}}^{\infty} \frac{1}{1+u^{\frac{\alpha}{2}}} du + \Psi(\chi) \right)} d\chi, \quad (43)$$

$$\text{where} \quad \Psi(\chi) = \frac{\rho e^{-\pi\lambda\tau^2} \psi_1(\chi) + \psi_2(\chi)}{\pi\lambda_i}. \quad (44)$$

To solve (43), we consider a lossy environment, where the path loss exponent $\alpha = 4$, we get

$$R_C^{(\hat{s})} = \int_0^{\infty} \frac{1}{(\chi + 1) \left(1 + \beta^{\frac{1}{2}} \left[\frac{\pi}{2} - \tan^{-1} \left(\beta^{-\frac{1}{2}} \right) \right] + \Psi(\chi) \right)} d\chi. \quad (45)$$

Similarly for D2D side, the successful probability and the data rate are derived and given by

$$P_{suc_{j_0}}^{(\hat{s})} = \exp(-\psi_d(\beta_d) x_{d_0}^2 \eta), \quad (46)$$

$$\text{and} \quad R_D^{(\hat{s})} = \int_0^{\infty} \frac{\exp(-\psi_d(\chi_d) x_{d_0}^2 \eta)}{(\chi_d + 1)} d\chi_d, \quad (47)$$

$$\text{where} \quad \eta = 1 + \rho e^{-\pi\lambda\tau^2} \sum_{j_1=1}^{N_{D_1}} \left[\xi_{j_1, j_0}^{\frac{2}{\alpha}} \right] + \sum_{j_2=1}^{N_{D_2}} \left[\xi_{j_2, j_0}^{\frac{2}{\alpha}} \right]. \quad (48)$$

Since the BS controls the number and location of DUEs in the protection band, thus the expected reuse factor of the protection band DRBs is denoted by r_{d-DDB} and can be found in terms of r_d as

$$r_{d-DDB} = \left\lfloor \rho e^{-\pi\lambda\tau^2} r_d \right\rfloor, \quad (49)$$

where $\lfloor \cdot \rfloor$ is the round down function.

Clearly, in this strategy, the total DUEs that can be served at each time slot can be reduced. To evaluate this reduction, we define a reduction percentage of the DUEs as a DDB strategy trade-off metric and derive it by calculating the number of DUEs that can be served for each case, when this strategy is employed and not employed. As a result, the reduction percentage is expressed by

$$\theta = \frac{N_D - \left(\rho e^{-\pi\lambda\tau^2} N_{D_1} + N_{D_2} \right)}{N_D} \times 100\%. \quad (50)$$

The DDB strategy defines a protection band to mitigate IEI. The main question is how to determine the optimal protection band size (DRBs groups setting) that maximizes the CUE coverage probability in (42)?. Intuitively, the maximum coverage probability can be achieved when the DRBs are not used by any DUEs, where ($\rho = 0$, $N_{D_1} = N_D$). For the efficient use of DRBs and to serve as much DUEs in each time slot, this is not an option. For this reason, we define ρ and the reduction percentage threshold θ_{th} as the QoS system parameters, where ρ is

selected to guarantee the efficient use of DRBs, and θ_{th} is the permitted reduction percentage that guarantees $N_{DUEs} = \theta_{th} \times r_d \times N_D$ DUEs can be served in one time slot t . The BS sets N_{DUEs} value according to: the number of DUEs requests in each time slot, and the system priorities of serving the DUEs or providing better QoS to the CUEs.

The BS finds the optimal protection band that maximizes the CUE coverage probability in (42) for a given reduction factor ρ , so as the reduction percentage θ does not exceed the given θ_{th} as follows. (42) is maximized by minimizing the third term in the dominator as

$$\underset{N_{D_1}}{\text{minimize}} \quad \frac{\rho e^{-\pi\lambda\tau^2} \psi_1(\beta) + \psi_2(\beta)}{\pi\lambda_i} \quad (51)$$

$$\text{subject to} \quad \frac{N_D - (\rho N_{D_1} + N_{D_2})}{N_D} \leq \theta_{th} \quad (51a)$$

$$1 \leq N_{D_1} \leq N_D. \quad (51b)$$

Since the N_{D_1} is the upper limit of a summation operator in (39) and (40), thus it is tractable to derive the optimal ρ^* for the given DRBs groups setting N_{D_1} and then find the optimal $N_{D_1}^*$ in terms of derived ρ^* . The problem can be rewritten as

$$\text{minimize} \quad \rho \quad (52)$$

$$\text{subject to} \quad \frac{N_D - (\rho N_{D_1} + N_{D_2})}{N_D} \leq \theta_{th} \quad (52a)$$

$$0 \leq \rho \leq 1. \quad (52b)$$

Worth noting that τ in (42) is discarded and substituted by $\tau = 0$, because from the results (see Fig. 8 in the results section), we notice the exclusion distance τ does not help to improve the CUE performance.

To solve (52), we use the Lagrangian multipliers method and find the Lagrangian function as

$$\mathcal{L}(\rho, \lambda_1, \lambda_2, \lambda_3) = \rho + \lambda_1 \left(\frac{N_D - (\rho N_{D_1} + N_{D_2})}{N_D} - \theta_{th} \right) + \lambda_2(\rho - 1) - \lambda_3\rho, \quad (53)$$

where λ_1 , λ_2 , λ_3 , and λ_4 are the Lagrangian multipliers. The gradients of Lagrangian function vanish at ρ^* , so we find partial derivations with respect of each variable ρ , λ_1 , λ_2 , and λ_3 as

$$\frac{\partial \mathcal{L}(\rho^*, \lambda_1^*, \lambda_2^*, \lambda_3^*)}{\partial \rho} = 1 - \frac{N_{D_1}}{N_D} \lambda_1^* + \lambda_2^* - \lambda_3^* = 0, \quad (54)$$

$$\frac{\partial \mathcal{L}(\rho^*, \lambda_1^*, \lambda_2^*, \lambda_3^*)}{\partial \lambda_1} = \frac{N_D - (\rho^* N_{D_1} + N_{D_2})}{N_D} - \theta_{th} = 0, \quad (55)$$

$$\frac{\partial \mathcal{L}(\rho^*, \lambda_1^*, \lambda_2^*, \lambda_3^*)}{\partial \lambda_2} = \rho^* - 1 = 0, \quad (56)$$

$$\frac{\partial \mathcal{L}(\rho^*, \lambda_1^*, \lambda_2^*, \lambda_3^*)}{\partial \lambda_3} = -\rho^* = 0. \quad (57)$$

From (55), we can find ρ^* as

$$\rho^* = \frac{N_D - N_{D_2} - N_D \theta_{th}}{N_{D_1}}, \quad (58)$$

where $\rho^* = 1$ in (56) is not the minimum value among the derived optimal solutions. Further, for the sake of spectrum efficiency, $\rho^* = 0$ in (57) is discarded. Thus, from (58), the optimal DRB setting can be obtained as

$$N_{D_1}^* = \frac{N_D \theta_{th}}{1 - \rho} \quad \text{where} \quad 0 < \rho < 1. \quad (59)$$

From (59), if we let $N_{D_1} = N_D$, we obtain maximum reduction can be achieved for a given ρ

$$\theta_{max} = 1 - \rho. \quad (60)$$

To leverage the fact that the center DUEs cause an interference higher than the edge DUEs to the BS, the DUEs are arranged by increasing order of the BS interference level. By exploiting the optimal protection band size derived in (59), the $(r_d - DDB \times N_{D_1})$ DUEs cause the lowest interference to the BS are allocated to G_1 band. The $(r_d \times N_{D_2})$ DUEs cause the highest interference to the BS are allocated to G_2 band. This frequency resources allocation mitigates the IEI. Thereafter, the DUEs allocated for each band G_1 and G_2 could be distributed by using the traditional resource allocation methods.

B. Optimal power allocation (OPA) algorithm for DUEs

From subsection A in the results section, the IEI intra-cell dominates the IEI inter-cell in high dense D2D-enabled cellular network. Thus, eliminating IEI intra-cell within one cell can diminish significantly the total IEI impact in the network. Therefore, the OPA algorithm is proposed to mitigate the IEI intra-cell using the fact that by controlling the DUEs transmission power within one cell, the IEI impact can be effectively controlled. This method can eliminate the IEI intra-cell because the BS can only control and allocate power to the DUEs within the cell. The optimal power allocation is performed for the DUEs that maximizes the DUEs sum rate and satisfies the required constraint in order to mitigate the IEI from the DUEs to the cellular links as

$$\underset{\mathbf{p}}{\text{maximize}} \quad \sum_{j=1}^{N_D} \sum_{\vartheta=1}^{r_j} R_{\vartheta}^j(\mathbf{P}) \quad (61)$$

$$\text{subject to} \quad P_{\vartheta}^j \leq P_{max}, \forall \vartheta \quad \text{and} \quad \forall j \quad (61a)$$

$$\sum_{\vartheta=1}^{r_j} P_{\vartheta}^j H_{\vartheta,BS}^j \leq I_{th}, \forall j. \quad (61b)$$

The objective function (61) is the DUEs sum rate within the cell, where \mathbf{p} denotes the transmission power profile vector for DUEs, R_{ϑ}^j is the data rate for ϑ th DUE that uses j th DRB, and r_j is number of DUEs that can reuse j th DRB, which is defined in the frequency resources allocation stage for each DRB. It is assumed that the spectrum allocation has been performed before the power allocation, where DRBs are allocated to subset of distant pairs that generates low interference to each others. Further, constraint (61a) guarantees that the transmit power for each DUE is less than or equal to the maximum limit, where P_{ϑ}^j is the ϑ th DUE transmission power that uses j th DRB, P_{max} is the maximum transmit power of the DUEs, $\vartheta \in \{1, 2, \dots, r_j\}$, and $j \in \{1, 2, \dots, N_D\}$. Finally, constraint (61b) guarantees the interference from the DUEs at the BS is less than a given threshold I_{th} . $H_{\vartheta,BS}^j$ denotes the channel gain between the ϑ th DUE that uses j th DRB and the BS, where $H_{\vartheta,BS}^j = h_{\vartheta,BS} x_{\vartheta}^{-\alpha}$. I_{th} is the maximum allowed interference from each DRB at the BS which controls the IEI from the DUEs.

For notation clarity, henceforth, the lower and upper symbols of rate R , power P , co-channel interference I , and IEI indicate the DUE identity and the DRB used by this DUE, respectively. Also, for channels notations, the upper symbol is the same as later, however, the lower symbol indicates that, for instance, channel $H_{\vartheta,BS}$ is between ϑ th DUE transmitter and BS receiver.

The data rate for ϑ_0 th DUE that uses j_0 th DRB can be written as

$$R_{\vartheta_0}^{j_0}(\mathbf{p}) = \ln \left(1 + \frac{P_{\vartheta_0}^{j_0} H_{\vartheta_0, \vartheta_0}^{j_0}}{I_{\vartheta_0}^{j_0} + IEI_{\vartheta_0}^{j_0} + \sigma^2} \right), \quad (62)$$

where

$$I_{\vartheta_0}^{j_0} = \sum_{\substack{\vartheta=1 \\ \vartheta \neq \vartheta_0}}^{r_j} P_{\vartheta}^{j_0} H_{\vartheta, \vartheta_0}^{j_0}, \quad (63)$$

and

$$IEI_{\vartheta_0}^{j_0} = \sum_{j=1}^{N_D} \sum_{\ell=1}^{r_j} P_{\ell}^j H_{\ell, \vartheta_0}^j \xi_{j, j_0}, \quad (64)$$

where $I_{\vartheta_0}^{j_0}$ and $IEI_{\vartheta_0}^{j_0}$ are the cumulative co-channel interference and cumulative IEI at j_0 DRB used by ϑ_0 th DUE within one cell.

The objective function (61) is non-convex function (geometric programming function) and the constraints are convex (affine functions). To simplify the problem and find the optimal solution, we convert (61) to a convex form as follows. By using the high SINR regime and replacing $P_{\vartheta_0}^{j_0}$ with $e^{(\hat{P}_{\vartheta_0}^{j_0})}$, we get

$$\sum_{j=1}^{N_D} \sum_{\mathfrak{d}=1}^{r_j} R_{\mathfrak{d}0}^{j0}(\mathbf{p}) = \sum_{j=1}^{N_D} \sum_{\mathfrak{d}=1}^{r_j} \left[\hat{P}_{\mathfrak{d}0}^{j0} + \ln(H_{\mathfrak{d}0,\mathfrak{d}0}^{j0}) - \ln \left(\sum_{\substack{\mathfrak{d}=1 \\ \mathfrak{d} \neq \mathfrak{d}_0}}^{r_j} e^{(\hat{P}_{\mathfrak{d}0}^{j0})} H_{\mathfrak{d},\mathfrak{d}0}^{j0} + \sum_{j=1}^{N_D} \sum_{\mathfrak{k}=1}^{r_j} e^{(\hat{P}_{\mathfrak{k}}^j)} H_{\mathfrak{k},\mathfrak{d}0}^j \xi_{j,j_0} + \sigma^2 \right) \right]. \quad (65)$$

The first term on the right hand side in (65) is linear and the third term is concave (the log of sum of exponentials of linear functions), then the transformed objective function (65) represents one form of convex functions and it has a unique optimal solution which must satisfy Karush-Kuhn-Tucker (KKT) conditions and can be solved by using Lagrangian dual decomposition. By letting $\vartheta = (\vartheta_1, \dots, \vartheta_i)$ and $\varpi = (\varpi_1, \dots, \varpi)$ denote the Lagrangian multiplier vectors associated with the constraints (61a) and (61b), respectively, the Lagrangian dual function can be defined as

$$\mathcal{L}(P_{\mathfrak{d}}^j, \vartheta, \varpi) = \sum_{j=1}^{N_D} \sum_{\mathfrak{d}=1}^{r_j} R_{\mathfrak{d}}^j(\mathbf{P}) - \sum_{j=1}^{N_D} \sum_{\mathfrak{d}=1}^{r_j} \vartheta_{\mathfrak{d}}^j (P_{\mathfrak{d}}^j - P_{max}) - \sum_{j=1}^{N_D} \varpi_j \left(\sum_{\mathfrak{d}=1}^{r_j} P_{\mathfrak{d}}^j H_{\mathfrak{d},BS}^j - I_{th} \right). \quad (66)$$

According to the KKT conditions [19], the gradient of the Lagrangian dual function must vanish at the optimum \mathbf{P}^* and equal to $\mathbf{0}$.

$$\frac{\partial \mathcal{L}(P_{\mathfrak{d}_0}^{j_0*}, \vartheta^*, \varpi^*)}{\partial P_{\mathfrak{d}_0}^{j_0}} = \sum_{j=1}^{N_D} \sum_{\mathfrak{d}=1}^{r_j} \frac{\partial R_{\mathfrak{d}}^j(\mathbf{P}^*)}{\partial P_{\mathfrak{d}_0}^{j_0}} - \vartheta_{\mathfrak{d}_0}^{j_0*} - \varpi_{j_0}^* H_{\mathfrak{d}_0,BS}^{j_0} = 0. \quad (67)$$

To derive (67), we firstly derive the first term on the right hand side. The transmission power of \mathfrak{d}_0 th DUE that uses j_0 th DRB $P_{\mathfrak{d}_0}^{j_0}$ can be found in the sum rate equation of DUEs in three forms as follows: in the desired signal of \mathfrak{d}_0 th DUE that uses j_0 th DRB, in the co-channel interference of \mathfrak{d}_0 th DUE to \mathfrak{d} th DUE that uses same j_0 th DRB, and in the IEI of \mathfrak{d}_0 th DUE to \mathfrak{k} th DUE that uses different DRB. This can be expressed mathematically as

$$\sum_{j=1}^{N_D} \sum_{\mathfrak{d}=1}^{r_j} \frac{\partial R_{\mathfrak{d}}^j(\mathbf{P}^*)}{\partial P_{\mathfrak{d}_0}^{j_0}} = \frac{\partial R_{\mathfrak{d}_0}^{j_0}(\mathbf{P}^*)}{\partial P_{\mathfrak{d}_0}^{j_0}} + \sum_{\substack{\mathfrak{d}=1 \\ \mathfrak{d} \neq \mathfrak{d}_0}}^{r_j} \frac{\partial R_{\mathfrak{d}}^{j_0}(\mathbf{P}^*)}{\partial P_{\mathfrak{d}_0}^{j_0}} + \sum_{\substack{j=1 \\ j \neq j_0}}^{N_D} \sum_{\substack{\mathfrak{k}=1 \\ \mathfrak{k} \neq \mathfrak{d}_0}}^{r_j} \frac{\partial R_{\mathfrak{k}}^j(\mathbf{P}^*)}{\partial P_{\mathfrak{d}_0}^{j_0}}, \quad (68)$$

and can be determined term by term as follows. The derivative of utility function $R_{\mathfrak{d}_0}^{j_0}$ with respect to $P_{\mathfrak{d}_0}^{j_0}$ is

$$\frac{\partial R_{\mathfrak{d}_0}^{j_0}(\mathbf{P}^*)}{\partial P_{\mathfrak{d}_0}^{j_0}} = \frac{1}{P_{\mathfrak{d}_0}^{j_0*}}. \quad (69)$$

The derivative of utility function $R_{\mathfrak{d}}^{j_0}$ with respect to $P_{\mathfrak{d}_0}^{j_0}$, with $\mathfrak{d}_0 \neq \mathfrak{d}$, is

$$\frac{\partial R_{\mathfrak{d}}^{j_0}(\mathbf{P}^*)}{\partial P_{\mathfrak{d}_0}^{j_0}} = -\frac{H_{\mathfrak{d}_0,\mathfrak{d}}^{j_0}}{I_{\mathfrak{d}}^{j_0}(\mathbf{P}^*) + IEI_{\mathfrak{d}}^{j_0}(\mathbf{P}^*) + \sigma^2}, \quad (70)$$

where

$$\begin{aligned}
 R_{\mathfrak{d}}^{j_0}(\mathbf{P}^*) &= \ln \left(\frac{P_{\mathfrak{d}}^{j_0} H_{\mathfrak{d},\mathfrak{d}}^{j_0}}{I_{\mathfrak{d}}^{j_0} + I E I_{\mathfrak{d}}^{j_0} + \sigma^2} \right) \\
 I_{\mathfrak{d}}^{j_0}(\mathbf{P}^*) &= P_{\mathfrak{d}_0}^{j_0} H_{\mathfrak{d}_0,\mathfrak{d}}^{j_0} + \sum_{\substack{\mathfrak{d}'=1 \\ \mathfrak{d}' \neq \mathfrak{d}}} P_{\mathfrak{d}'}^{j_0} H_{\mathfrak{d}',\mathfrak{d}}^{j_0} \\
 I E I_{\mathfrak{d}}^{j_0}(\mathbf{P}^*) &= \sum_{\substack{j=1 \\ j \neq j_0}}^{N_D} \sum_{\mathfrak{k}=1}^{r_j} P_{\mathfrak{k}}^j H_{\mathfrak{k},\mathfrak{d}}^j \xi_{j,j_0},
 \end{aligned}$$

and $R_{\mathfrak{k}}^j$ with respect to $P_{\mathfrak{d}_0}^{j_0}$, with $j \neq j_0$, is

$$\frac{\partial R_{\mathfrak{k}}^j(\mathbf{P}^*)}{\partial P_{\mathfrak{d}_0}^{j_0}} = - \frac{H_{\mathfrak{d}_0,\mathfrak{k}}^{j_0}}{I_{\mathfrak{k}}^j(\mathbf{P}^*) + I E I_{\mathfrak{k}}^j(\mathbf{P}^*) + \sigma^2}, \quad (71)$$

where

$$\begin{aligned}
 R_{\mathfrak{k}}^j(\mathbf{P}^*) &= \ln \left(\frac{P_{\mathfrak{k}}^j H_{\mathfrak{k},\mathfrak{k}}^j}{I_{\mathfrak{k}}^j(\mathbf{P}^*) + I E I_{\mathfrak{k}}^j(\mathbf{P}^*) + \sigma^2} \right) \\
 I_{\mathfrak{k}}^j(\mathbf{P}^*) &= \sum_{\substack{\mathfrak{d}=1 \\ \mathfrak{d} \neq \mathfrak{k}}}^{r_j} P_{\mathfrak{d}}^j H_{\mathfrak{d},\mathfrak{k}}^j \\
 I E I_{\mathfrak{k}}^j(\mathbf{P}^*) &= P_{\mathfrak{d}_0}^{j_0} H_{\mathfrak{d}_0,\mathfrak{k}}^{j_0} + \sum_{\substack{j_0=1 \\ j_0 \neq j}}^{N_D} \sum_{\substack{\mathfrak{d}''=1 \\ \mathfrak{d}'' \neq \mathfrak{d}_0}}^{r_j} P_{\mathfrak{d}''}^{j_0} H_{\mathfrak{d}'',\mathfrak{k}}^{j_0} \xi_{j_0,j}.
 \end{aligned}$$

By substituting (69), (70), and (71) in (68), and then in (67), we get

$$\begin{aligned}
 \frac{\partial \mathcal{L}(P_{\mathfrak{d}_0}^{j_0*}, \vartheta^*, \varpi^*)}{\partial P_{\mathfrak{d}_0}^{j_0}} &= \frac{1}{P_{\mathfrak{d}_0}^{j_0*}} - \sum_{\substack{\mathfrak{d}=1 \\ \mathfrak{d} \neq \mathfrak{d}_0}}^{r_j} \frac{H_{\mathfrak{d}_0,\mathfrak{d}}^{j_0}}{I_{\mathfrak{d}}^{j_0}(\mathbf{P}^*) + I E I_{\mathfrak{d}}^{j_0}(\mathbf{P}^*) + \sigma^2} \\
 &\quad - \sum_{\substack{j=1 \\ j \neq j_0}}^{N_D} \sum_{\substack{\mathfrak{k}=1 \\ \mathfrak{k} \neq \mathfrak{d}_0}}^{r_j} \frac{H_{\mathfrak{d}_0,\mathfrak{k}}^{j_0}}{I_{\mathfrak{k}}^j(\mathbf{P}^*) + I E I_{\mathfrak{k}}^j(\mathbf{P}^*) + \sigma^2} - \vartheta_{\mathfrak{d}_0}^{j_0*} - \varpi_{j_0}^* H_{\mathfrak{d}_0,BS}^{j_0} = 0.
 \end{aligned} \quad (72)$$

From (72), the optimal power allocation for each \mathfrak{d} th DUE on each j th DRB is derived as follows

$$P_{\mathfrak{d}_0}^{j_0*} = \frac{1}{f_{\mathfrak{d}_0}^{j_0}(\mathbf{P}^*, \vartheta^*, \varpi^*)}, \quad (73)$$

where

$$\begin{aligned}
 f_{\mathfrak{d}_0}^{j_0}(\mathbf{P}^*, \vartheta^*, \varpi^*) &= \sum_{\substack{\mathfrak{d}=1 \\ \mathfrak{d} \neq \mathfrak{d}_0}}^{r_j} \frac{H_{\mathfrak{d}_0,\mathfrak{d}}^{j_0}}{I_{\mathfrak{d}}^{j_0}(\mathbf{P}^*) + I E I_{\mathfrak{d}}^{j_0}(\mathbf{P}^*) + \sigma^2} \\
 &\quad + \sum_{\substack{j=1 \\ j \neq j_0}}^{N_D} \sum_{\substack{\mathfrak{k}=1 \\ \mathfrak{k} \neq \mathfrak{d}_0}}^{r_j} \frac{H_{\mathfrak{d}_0,\mathfrak{k}}^{j_0}}{I_{\mathfrak{k}}^j(\mathbf{P}^*) + I E I_{\mathfrak{k}}^j(\mathbf{P}^*) + \sigma^2} + \vartheta_{\mathfrak{d}_0}^{j_0*} + \varpi_{j_0}^* H_{\mathfrak{d}_0,BS}^{j_0}.
 \end{aligned} \quad (74)$$

Since the Lagrangian dual function in (66) is differentiable, sub-gradient method can be used to find optimal power profile, where convergence of this method is guaranteed. By using the

Algorithm 1 Optimal power control algorithm

- 1: Initialize \mathfrak{T} , $\vartheta_{\mathfrak{d}_0}^{j_0}(\mathfrak{T}) \quad \forall \mathfrak{d}_0 \in \{1, \dots, r_j\} \wedge \forall j_0 \in \{1, \dots, N_D\}$, and $\varpi_{j_0}(\mathfrak{T}) \quad \forall j_0 \in \{1, \dots, N_D\}$ with zero value. Initialize \mathbf{P} with equal power allocation.
 - 2: Calculate $P_{\mathfrak{d}_0}^{j_0} \quad \forall \mathfrak{d}_0 \in \{1, \dots, r_j\} \wedge \forall j_0 \in \{1, \dots, N_D\}$ using equation (73).
 - 3: Update $\vartheta_{\mathfrak{d}_0}^{j_0}(\mathfrak{T}) \quad \forall \mathfrak{d}_0 \in \{1, \dots, r_j\} \wedge \forall j_0 \in \{1, \dots, N_D\}$, $\varpi_{j_0}(\mathfrak{T}) \quad \forall j_0 \in \{1, \dots, N_D\}$ using equation (75), and \mathbf{P} .
 - 4: Until $\mathfrak{T} = \mathfrak{T}_{max}$ (max number of iteration).
-

constant step size rule, the Lagrange multipliers can be updated iteratively until convergence by

$$(\vartheta_{\mathfrak{d}_0}^{j_0})^{\mathfrak{T}+1} = \left[(\vartheta_{\mathfrak{d}_0}^{j_0})^{\mathfrak{T}} - a(P_{max} - P_{\mathfrak{d}_0}^{j_0}) \right]^+, \quad (75a)$$

$$(\varpi_{j_0})^{\mathfrak{T}+1} = \left[(\varpi_{j_0})^{\mathfrak{T}} - b \left(I_{th} - \sum_{\mathfrak{d}_0=1}^{r_j} P_{\mathfrak{d}_0}^{j_0} H_{\mathfrak{d}_0, BS}^{j_0} \right) \right]^+, \quad (75b)$$

where $[x]^+$ denotes $\max\{x, 0\}$, $a > 0$ and $b > 0$ are small positive steps, and \mathfrak{T} is the iteration index. Algorithm 1 is developed to derive the optimal power allocations for DUEs. It is worth noting that the algorithm's complexity is polynomial in mean of r_j over all DRBs (\bar{r}_j), N_D , and the iteration $O(\bar{r}_j \times N_D \times \mathfrak{T}_{max})$, which is feasible in practice with reasonable processing delay. The proposed algorithm is mainly based on knowing the channel gains of different links between various devices (CUEs, DUEs, and BS). Also, it is worth noting that the channel gains among the DUEs and CUEs, and the BS can be obtained in a practical network by using the uplink sounding reference signal (SRS), for more details refer to [20].

V. RESULTS AND DISCUSSION

This section provides the numerical and simulation results for D2D-enabled cellular network. The results are all averaged over the CRBs by using (14) and averaged over the DRBs by using (23). Unless noted otherwise, the simulation parameters are given in Table. I. Leakage power ratio among the resource blocks is given by $\xi_{j,i} = -21 - 5|j - i|$ in dB [8].

A. IEI impact

In this subsection, we compare no IEI case in [21], [22], and [23] with the IEI case. The results show the IEI impact on cellular and D2D links, the dominant IEI (intra-cell or inter-cell), and the comparison between the reuse factors, where IEI is taken and not taken into account.

Fig. 4 shows the IEI impact on the CUE coverage probability for different DUE densities by changing the required SINR threshold at the reference BS. The coverage probability is calculated

TABLE I: Simulation Parameters

Parameters	Values
Number of DRBs N_D	44 [24], [25]
Number of CRBs N_C	6 [24], [25]
DRBs indices j	4 to 47 [24], [25]
CRBs indices i	from 1 to 3,48 to 50
CUE transmission power P_C for $\epsilon = 0$	23 dBm
DUE transmission power P_D	20 dBm
BS and CUE Density λ, λ_i	1 (BS, CUEs)/km ²
Path loss exponent α	4
BS SINR threshold β	-5 dB
DUE SINR threshold β_d	0 dB
Network Radius	5 km
D2D typical link distance x_{d_0}	50 m
Operating frequency	2 GHz

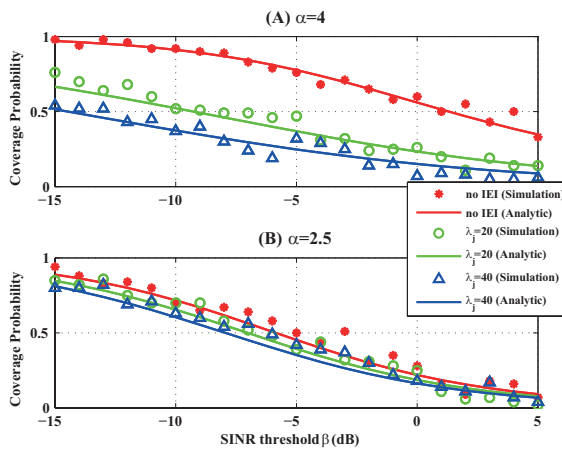


Fig. 4: IEI impact on the CUEs in the network.

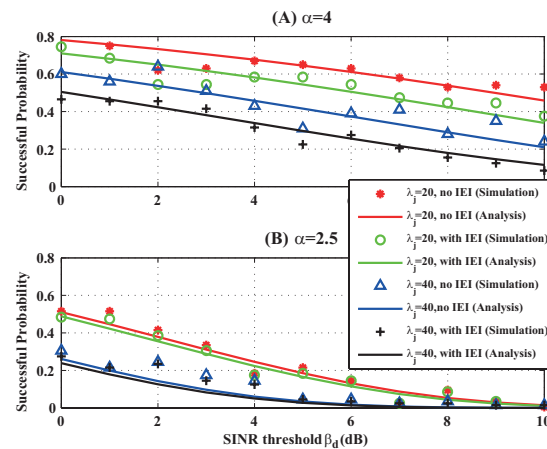


Fig. 5: IEI impact on the DUEs in the network.

by considering two different environment: lossy environment $\alpha = 4$ and free space environment $\alpha = 2.5$. To find the CUE coverage probability by simulations, the typical BS is located at the center $(0, 0)$ in \mathbb{R}^2 plane. The CUEs are dropped according to homogeneous PPP with density $\lambda_i = 1$ CUEs/km² within the range of 5 km of the network, and the same for the DUEs with different densities. The figure shows the simulation results capture the coverage probability in (13). By comparing the $\lambda_j = 20$ and 40 DUEs/km² scenarios with no IEI scenario, it can be seen that the IEI degrades the coverage probability and becomes severe by increasing the density. Since the DUE density is expected to increase dramatically in the next generation networks, the IEI becomes severe, thus, the system should consider the IEI to evaluate the network performance accurately. Further, the IEI degrades the coverage probability by 0.4 and 0.5 for $\alpha = 4$, while for $\alpha = 2.5$ case, coverage is degraded by 0.1 and 0.2, where $\lambda_j = 20$ and 40 DUEs/km² respectively. This leads to conclude that IEI impact is more significant in lossy environment.

Fig. 5 shows the IEI impact on the DUE successful probability for different DUE densities by changing the required SINR threshold at the reference DUE receiver. To find the DUE successful probability by simulation, the reference DUE receiver is centred at the origin, the corresponding typical DUE transmitter is isotropically dropped at a fixed distance $x = 50$ m away from the receiver. The CUEs and DUEs are dropped around the center according to homogeneous PPP. The successful probability is calculated for lossy environment $\alpha = 4$ and free space environment $\alpha = 2.5$. The figure shows the simulation results capture the successful probability in (22). From $\lambda_j = 20$ and 40 DUEs/km² scenarios, it can be seen that the IEI degrades the D2D link successful probability. The IEI degrades the successful probability by about 0.1, where $\lambda_j = 20$ and 40 DUEs/km² for $\alpha = 4$ case, while for $\alpha = 2.5$ case the IEI does not affect the successful probability and it is almost similar to the no IEI case. By increasing the DUE density, the IEI slightly increases and a negligible effect on successful probability is caused. This leads to conclude that the IEI impact for D2D side is not severe. Further, the IEI impact is higher in the lossy environment, which means the overall interference is smaller in proportion to the desired received signal for the former case. The reason is the D2D communication distance between the transmitter and the receiver of D2D pair is small.

Fig. 6 shows the coverage probability where: only IEI intra-cell, only IEI inter-cell, and the IEI for whole network are considered, respectively. Three cases are defined for two different frequency resources pool structures, $N_C = 20, N_D = 30$ and $N_C = 6, N_D = 44$ by changing DUE density. Note that the coverage probability for $\lambda_j = 0$ is 0.77 represents no IEI case (optimal case). By changing DUE density, we observe that IEI intra-cell is significantly high and affects the coverage probability of typical CUE for $N_C = 6, N_D = 44$ and $N_C = 20, N_D = 30$ cases. The reason is the proximity of interferer DUEs of typical cell from the reference BS. However for both cases, the IEI inter-cell is not negligible especially at high DUE density. As a result, the IEI intra-cell dominates the performance at high DUE density. At low DUE density, both similarly affect the coverage probability. This implies, considering only IEI intra-cell in high DUE density can help to evaluate approximately the cellular system performance, especially if the BS has limited information about the IEI from the other cells. Since the full load scenario is considered, by comparing the $N_C = 6, N_D = 44$ curves and $N_C = 20, N_D = 30$ curves, it can be seen the coverage probability is better when the DRBs number is less.

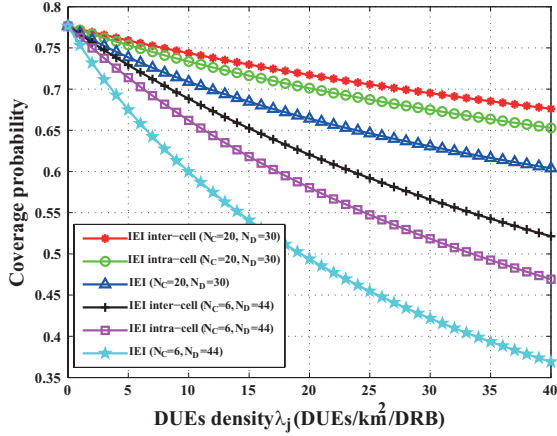


Fig. 6: IEI intra-cell and IEI inter-cell.

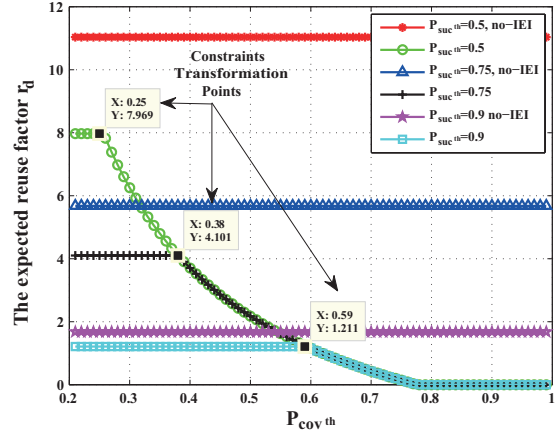


Fig. 7: Expected reuse factor for no IEI and IEI cases.

Fig. 7 shows the expected reuse factor for each DRB, where the required CUE coverage probability at the BS and the DUE successful probability are given. In this figure, the expected DRBs reuse factor is calculated for no IEI and IEI to show the difference between two cases. It can be seen, if the required coverage probability threshold is small and reuse factor that satisfies the coverage probability threshold is larger than reuse factor that satisfies the successful probability threshold, then the expected reuse factor is bounded by successful probability constrain (33b). The vice versa, for the large coverage probability threshold, in this case, optimal reuse factor is bounded by the coverage probability constrain (33a). The points of the transformation between two above cases are defined as the constraints transformation points as shown in the figure. Further, the number of expected reuse factor for no IEI case is greater than the actual expected reuse factor for the IEI case. For instance, if the required P_{suc}^{th} is 0.5, the expected reuse factor is 11, which is not an accurate because if the IEI is considered we notice that the maximum reuse factor can be achieved is 8. As the result, the expected number of the DUEs that can be served in each time slot is calculated for no IEI and IEI cases, and the calculated number for the IEI can give a more accurate insight of how many DUEs can be served in each time slot without causing a harmful interference among the UEs, especially at the high DUE density.

B. IEI mitigation: DDB strategy

In this subsection, the results show the performance gain when the DDB strategy is employed and the optimal DRBs groups setting for different reduction factors that retains the reduction percentage less than the threshold value. The simulation setting is similar to the setting in the previous section, except the DUEs that use G_1 DRBs are dropped according to homogeneous

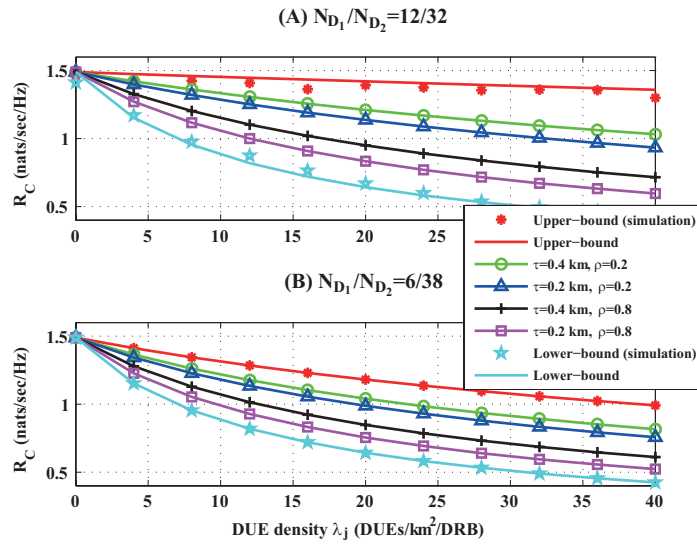


Fig. 8: Performance improvement of the DDB strategy.

PPP with density $\rho\lambda_j$, and beyond the exclusion distance τ from the BSs in the network.

Fig. 8 shows the expected cellular link data rate that can be achieved by employing DDB strategy for different DUE densities, DRBs groups setting, and different ρ and τ values. The figure demonstrates the lower-bound (no mitigation) and the upper-bound of the data rate for two different DRBs groups setting. For the upper-bound case, the G_1 DRBs are not used by any DUEs where $\rho = 0$, the data rate is improved significantly especially when the number of the DRBs in G_1 is large. For instance, for $N_{D_1} = 12$ case, the upper bound data rate is almost the same as the calculated data rate for the optimal case (no IEI) $R_C = 1.48$ nats/sec/Hz. For the same DRBs groups setting N_{D_1} and reduction factor ρ , if we increase the exclusion distance from 0.2 to 0.4 km, the improvement is only about 0.1 nats/sec/Hz, which is marginal and not a very promising enhancement. Further, for the same τ and ρ , if we increase the G_1 DRBs from 6 to 12 DRBs, the improvement is significant, particularly if the reduction factor is small. Also, we observe that the data rate increases when the reduction factor decreases for the same τ and N_{D_1} , which becomes notable if N_{D_1} is large. This figure shows that by decreasing the number of DUEs use G_1 DRBs and by increasing the number of DRBs in G_1 , we can effectively mitigate the IEI and achieve a significant improvement in performance. On the other hand, the exclusion distance τ plays a very marginal rule in this improvement.

In Fig. 9, the cellular link coverage probability is found for different DRBs groups settings and reduction factors. The coverage probability becomes better by increasing the number of the DRBs and the reduction factor in G_1 . Intuitively, the maximum coverage probability can be

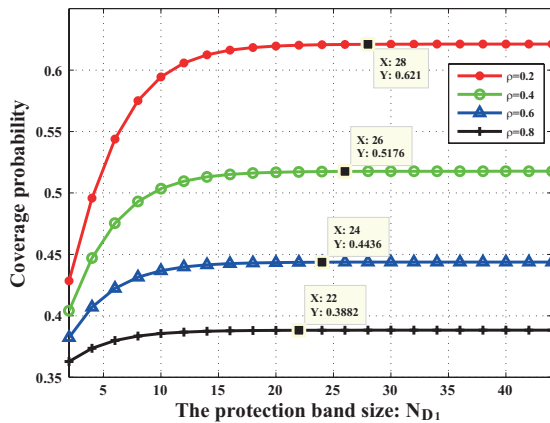


Fig. 9: Coverage probability with upper bound DRBs group setting points for $\lambda_j = 40$.

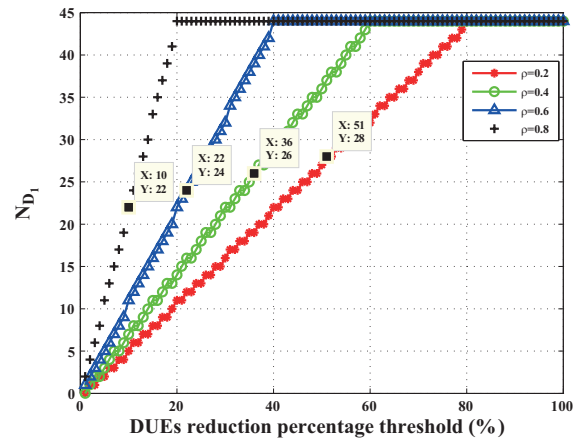


Fig. 10: Optimal DRBs groups setting for $\lambda_j = 40$ DUEs/km².

achieved where the reduction is applied for all DRBs, but this is not the case here, the maximum coverage probabilities for $\rho = 0.2, 0.4, 0.6$, and 0.8 can be achieved when the DRBs group setting N_{D_1} are $30, 28, 24$, and 22 , respectively. Increasing N_{D_1} after these points cannot achieve better performance. The main reason is the leakage from the DRBs located far from the CRBs is very small and negligible. This figure defines the upper bound DRBs group setting points for the given ρ , which helps to find the optimal DRBs groups setting as will be explained next.

Fig. 10 shows the optimal DRBs groups setting for the given reduction percentage and reduction factor. On this figure, we define the upper bound DRBs groups setting points. These points define the maximum DRBs groups setting and reduction that can be employed for each ρ . Accordingly, the DRBs groups setting can be found easily for the given ρ and reduction percentage by knowing the upper bound DRBs group setting points. For instance, for $\rho = 0.2$, if the allowable reduction percentage is 40% , then the DRBs groups setting $N_{D_1} = 22$. Meanwhile, if the allowable reduction percentage is $\geq 51\%$ then the DRBs groups setting is $N_{D_1} = 28$, which is equal to the upper bound DRBs groups setting point. Further, it can be seen that the maximum reduction percentages for the given reuse factors are 80% for $\rho = 0.2$, 60% for $\rho = 0.4$, 40% for $\rho = 0.6$, and 20% for $\rho = 0.8$, which also can be obtained by the derived equation in (60).

Accordingly, by knowing reduction factor, required reduction percentage, and upper bound DRBs group setting points, we can find optimal DRBs groups setting that minimises IEI impact within cell.

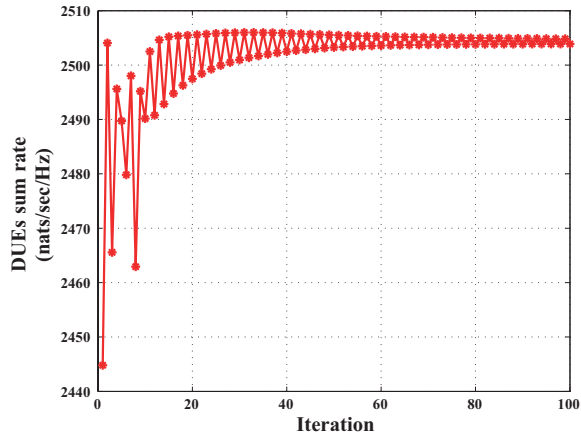


Fig. 11: Convergence performance of OPA algorithm for 352 DUEs/t, $I_{th}=0\text{dBm}$, and $N_D=44$ DRBs.

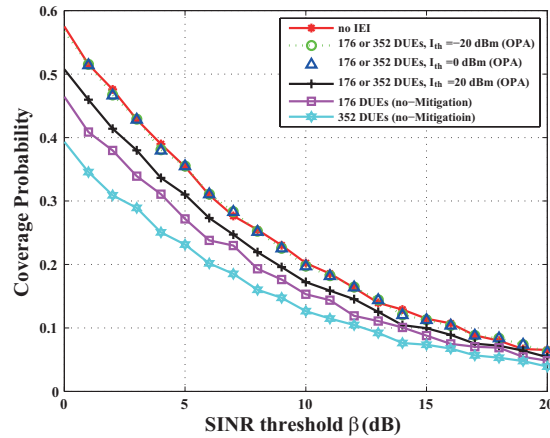


Fig. 12: Coverage probability improvement for OPA algorithm.

C. IEI mitigation: OPA algorithm

For OPA algorithm, we consider only one cell. This subsection depicts the convergence performance of the algorithm and the improvement achieved by employing OPA algorithm. The frequency resources allocation is performed before the power allocation by employing the DSATUR algorithm: If the distance between DUE transmitter ϑ th and DUE receiver ϑ' th is lower than a threshold distance then ϑ th and ϑ' th DUEs use different DRBs [26].

Fig. 11 illustrates the performance and shows the convergence behaviour of the OPA algorithm. The convergence to the maximum sum rate is achieved in iteration number 20. In this figure, the convergence for this algorithm is confirmed, which implies the maximum sum rate can be guaranteed by the OPA algorithm.

Fig. 12 shows the significant improvement in cellular link coverage probability that achieved by OPA algorithm. Three cases are compared: no IEI (optimal), no mitigation, and IEI. It can be seen that when the BS interference threshold I_{th} is decreased, the cellular link coverage probability can be improved and can achieve the optimal value. This is reasonable, because by decreasing I_{th} , the power profile of DUEs decreases. This causes less leakage power to the CRBs, thus the coverage probability becomes better. As a result, by exploiting the OPA algorithm, we can mitigate the IEI in D2D-enabled cellular network.

D. The mitigation methods comparison and its applications

In this paper, two different methods proposed to mitigate the IEI. In this section, we explain the application scenario of each method and compare them with the literature schemes.

1
2
3
4
5 DDB strategy serves limited number of DUEs with fix DUEs transmission power. The DDB
6 strategy can be used if the D2D links QoS has higher priority than the number of DUEs should
7 be served in each time slot and the DUEs requests for one time slot can be covered by this
8 strategy. By employing DDB strategy, the IEI intra-cell and IEI inter-cell can be mitigated.
9 Unlike the frequency resources grouping method proposed in [7], the DDB strategy mitigates
10 the IEI in all time slots without restricting the DUEs transmission power of the DUEs. Further,
11 by comparing with the OLPC-based methods proposed in [8]–[12], the DDB does not apply any
12 power transmission constraints on the DUEs, thus maintains the D2D links QoS.
13
14
15
16
17

18 The OPA algorithm applies power transmission constraints on the DUEs, while maximizes the
19 DUEs sum rate. This algorithm can be used if the number of served DUEs in each time slot has
20 higher priority than the D2D links QoS. By employing OPA algorithm: the DUEs transmission
21 power is controlled and the IEI intra-cell within one cell is mitigated. Unlike the power control
22 methods proposed in [8]–[12], OPA algorithm mitigates the IEI by taking into account the D2D
23 links as the cellular links QoS in the network, where the DUEs optimal power profile is found
24 which maximizes the DUEs sum rate and satisfies the interference threshold level at the BS.
25
26
27
28
29

30 As noted, it is preferable to use the DDB strategy if the required number of served DUEs in
31 one time slot can be covered. The main reason, in this strategy, the IEI is mitigated by taking into
32 account the D2D as the cellular links QoS. Also, there is no constraints on the DUEs transmission
33 power, and the IEI intra-cell and IEI inter-cell are both mitigated. In case the required number
34 of served DUEs in one time slot cannot be covered by DDB, the OPA algorithm can be used.
35
36
37
38

39 VI. CONCLUSION

40 This paper investigated IEI impact in high dense D2D-enabled cellular network. A new
41 framework was proposed to analyse accurately the future networks, which is more accurate
42 than traditional model, where IEI is taken into account. The results showed that the IEI affects
43 significantly network performance in particular cellular links. The frequency resources grouping
44 (DDB) strategy and optimal power allocation (OPA) algorithm were proposed to mitigate IEI
45 for cellular links in the network. The DDB strategy can be used if D2D links QoS has higher
46 priority than the number of DUEs should be served in each time slot and the DUEs requests
47 for one time slot can be covered by this strategy. Meanwhile, OPA algorithm can be used if the
48 number of served DUEs in each time slot has higher priority than the D2D links QoS and the
49 DUEs requests for one time slot cannot be covered by DDB strategy. The results showed that
50 the proposed methods mitigate IEI and improve remarkably cellular links performance.
51
52
53
54
55
56
57
58
59
60

APPENDIX A : PROOF OF $\mathcal{L}_{I_i}(s)$ DERIVATION

$$\begin{aligned}
\mathcal{L}_{I_i}(s) &= \mathbb{E}_{I_i}[\exp(-sI_i)] = \mathbb{E}_{R_m, \Phi_i, h_m} \left[\exp \left(-s \sum_{m \in \Phi_i/0} P_C R_m^{\alpha \epsilon} h_m x_m^{-\alpha} \right) \right] \\
&\stackrel{(a)}{=} \mathbb{E}_{R_m, \Phi_i} \left[\prod_{m \in \Phi_i/0} \mathbb{E}_{h_m} [\exp(-s P_C R_m^{\alpha \epsilon} h_m x_m^{-\alpha})] \right] \stackrel{(b)}{=} \mathbb{E}_{R_m, \Phi_i} \left[\prod_{m \in \Phi_i/0} \mu \int_0^\infty e^{-h(s P_C R_m^{\alpha \epsilon} x_m^{-\alpha} + \mu)} dh \right] \\
&\stackrel{(c)}{=} \mathbb{E}_{R_m} \left[\exp \left(-2\pi \lambda_i \int_{x_0}^\infty \left[\left(1 - \frac{\mu}{s P_C R_m^{\alpha \epsilon} x_m^{-\alpha} + \mu} \right) x_m dx_m \right] \right) \right] \\
&\stackrel{(d)}{=} \exp \left(-2\pi \lambda_i \int_{x_0}^\infty \frac{x_m}{1 + \left(\frac{\mu^{\frac{1}{\alpha}} x_m}{(s P_C \mathbb{E}_{R_m} [R_m^{\alpha \epsilon}])^{\frac{1}{\alpha}}} \right)^\alpha} dx_m \right). \tag{A1}
\end{aligned}$$

where (a) follows from the (i.i.d.) distribution of h_m and the independence from R_m , and PPP Φ_i , (b) follows from the fact that $h_m \sim \exp(\mu)$, (c) follows from the independence PPP Φ_i from R_m and the PGFL of PPP Φ_i [18], and (d) follows from the independence of R_m . Letting $u = \left(\frac{\mu^{\frac{1}{\alpha}} x_m}{(s P_C \mathbb{E}_{R_m} [R_m^{\alpha \epsilon}])^{\frac{1}{\alpha}}} \right)^2$, we get

$$\mathcal{L}_{I_i}(s) = \exp \left(-\pi \lambda_i \left(\frac{\mu}{s P_C \mathbb{E}_{R_m} [R_m^{\alpha \epsilon}]} \right)^{-\frac{2}{\alpha}} \int_{u(x_0)}^\infty \frac{1}{1 + u^{\frac{\alpha}{2}}} du \right). \tag{A2}$$

APPENDIX B : PROOF OF $\mathcal{L}_{IEI_i}(s)$ DERIVATION

$$\begin{aligned}
\mathcal{L}_{IEI_i}(s) &= \mathbb{E}_{IEI_i}[\exp(-sIEI_i)] = \mathbb{E}_{\Phi_j, h_{k,j}} \left[\exp \left(-s \sum_{j=1}^{N_D} \sum_{k \in \Phi_j} P_D h_{k,j} x_{k,j}^{-\alpha} \xi_{j,i} \right) \right] \\
&\stackrel{(a)}{=} \mathbb{E}_{\Phi_j} \left[\prod_{j=1}^{N_D} \prod_{k \in \Phi_j} \mathbb{E}_{h_{k,j}} \exp(-s P_D h_{k,j} x_{k,j}^{-\alpha} \xi_{j,i}) \right] \stackrel{(b)}{=} \mathbb{E}_{\Phi_j} \left[\prod_{j=1}^{N_D} \prod_{k \in \Phi_j} \int_0^\infty \mu e^{-h(\mu + s P_D x_{k,j}^{-\alpha} \xi_{j,i})} dh \right] \\
&\stackrel{(c)}{=} \prod_{j=1}^{N_D} \prod_{k \in \Phi_j} \mathbb{E}_{\Phi_j} \left[\frac{\mu}{\mu + s P_D x_{k,j}^{-\alpha} \xi_{j,i}} \right] \stackrel{(d)}{=} \prod_{j=1}^{N_D} \exp \left(-2\pi \lambda_j \int_0^\infty \left(1 - \frac{\mu}{\mu + s P_D x^{-\alpha} \xi_{j,i}} \right) x dx \right) \\
&\stackrel{(e)}{=} \prod_{j=1}^{N_D} \exp \left(-2\pi \lambda_j \left(\frac{\mu}{s P_D \xi_{j,i}} \right)^{-\frac{2}{\alpha}} \int_0^\infty \frac{v}{1 + v^\alpha} dv \right) \stackrel{(f)}{=} \prod_{j=1}^{N_D} \exp \left(-\frac{2\pi^2}{\alpha \sin \frac{2\pi}{\alpha}} \lambda_j \left(\frac{\mu}{s P_D \xi_{j,i}} \right)^{-\frac{2}{\alpha}} \right) \\
&\stackrel{(g)}{=} \exp \left(-\frac{2\pi^2}{\alpha \sin \frac{2\pi}{\alpha}} \lambda_j \left(\frac{\mu}{s P_D} \right)^{-\frac{2}{\alpha}} \sum_{j=1}^{N_D} \left[\xi_{j,i}^{\frac{2}{\alpha}} \right] \right), \tag{B1}
\end{aligned}$$

30

where (a) follows from the i.i.d distribution of $h_{k,j}$, and the independence from PPP Φ_j , (b) follows from $h \sim \exp(\mu)$, (c) follows from the independence of PPP Φ_j , (d) follows from the PGFL of PPP Φ_j , where the integration limits are from 0 to ∞ since the closest DUEs using the j th DRB are at least at a distance 0 from the reference BS, (e) follows from substitution $v^\alpha = \frac{\mu x^\alpha}{s P_D \xi_{j,i}}$, (f) follows from using [27, 3.241-2], and (g) follows from fairness assumption validation, where λ_j is equal for all DRBs.

REFERENCES

- [1] H. Albasry, H.Zhu, and J.Wang, "The Impact of In-band Emission Interference in D2D-Enabled Cellular Networks," in *IEEE Global Communications Conference (GLOBECOM)*, Singapore, December 2017, pp. 1–5.
- [2] H. Albasry and J. Wang, "Assessing and Mitigating the In-Band Emission Interference in D2D-Enabled Cellular Networks," in *IEEE 86th Vehicular Technology Conference (VTC Fall)*, Toronto, Canada, September 2017, pp. 1–5.
- [3] H. Albasry, "The Effect of D2D Communication on the Uplink Cellular Network Performance," in *IEEE 86th Vehicular Technology Conference (VTC Fall)*, Toronto, Canada, September 2017, pp. 1–5.
- [4] M. Azam, M. Ahmad, M. Naeem, M. Iqbal, A. Khwaja, A. Anpalagan, and S. Qaisar, "Joint admission control, mode selection and power allocation in D2D communication systems," *IEEE Transactions on Vehicular Technology*, vol. PP, no. 99, pp. 1–1, 2015.
- [5] H. ElSawy, E. Hossain, and M. Alouini, "Analytical modeling of mode selection and power control for underlay D2D communication in cellular networks," *IEEE Transactions on Communications*, vol. 62, no. 11, pp. 4147–4161, November 2014.
- [6] 3GPP TR 38.913, "Study on scenarios and requirements for next generation access technologies," February 2016.
- [7] D. Kim, Y. Kwak, J. Oh, Y. Kim, and J. Lee, "Discovery resource grouping for D2D discovery for mitigation of in-band emission in LTE-Advanced," in *IEEE Globecom Workshops (GC Wkshps)*, Austin, USA, December 2014, pp. 869–874.
- [8] Y. Kwak, S. Ro, S. Kim, Y. Kim, and J. Lee, "Performance evaluation of D2D discovery with eNB based power control in LTE-advanced," in *IEEE 80th Vehicular Technology Conference (VTC Fall)*, Vancouver, Canada, September 2014, pp. 1–5.
- [9] D. Li and Y. Liu, "In-band emission in LTE-A D2D: impact and addressing schemes," in *IEEE 81st Vehicular Technology Conference (VTC Spring)*, Glasgow, UK, May 2015, pp. 1–5.
- [10] W. Hwang, D. Lee, and H. Choi, "A new channel structure and power control strategy for D2D discovery in LTE cellular network," in *IEEE Asia-Pacific Conference on Communications (APCC)*, Pattaya, Thailand, October 2014, pp. 150–155.
- [11] J. Song, D. Lee, W. Hwang, and H. Choi, "A selective transmission power boosting method for D2D discovery in 3GPP LTE cellular system," in *IEEE International Conference on Information and Communication Technology Convergence (ICTC)*, Busan, Korea, October 2014, pp. 267–268.
- [12] H. Albasry and Q. Z. Ahmed, "Network-Assisted D2D discovery method by using efficient power control strategy," in *IEEE 83rd Vehicular Technology Conference (VTC Spring)*, Nanjing, China, May 2016, pp. 1–5.
- [13] H. Zhu and J. Wang, "Chunk-based resource allocation in OFDMA systems - part I: chunk allocation," *IEEE Transactions on Communications*, vol. 57, no. 9, pp. 2734–2744, September 2009.
- [14] H. Zhu, "Radio resource allocation for OFDMA systems in high speed environments," *IEEE Journal on Selected Areas in Communications*, vol. 30, no. 4, pp. 748–759, May 2012.
- [15] H. Zhu and J. Wang, "Chunk-based resource allocation in OFDMA systems - part II: joint chunk, power and bit allocation," *IEEE Transactions on Communications*, vol. 60, no. 2, pp. 499–509, February 2012.
- [16] H. Haas and S. McLaughlin, "A derivation of the PDF of adjacent channel interference in a cellular system," *IEEE Communications Letters*, vol. 8, no. 2, pp. 102–104, February 2004.
- [17] S. N. Chiu, D. Stoyan, W. S. Kendall, and J. Mecke, *Stochastic geometry and its applications*. John Wiley & Sons, 2013.
- [18] M. Haenggi, "Stochastic geometry for wireless networks," 2013.
- [19] S. Boyd and L. Vandenberghe, *Convex optimization*. Cambridge university press, 2004.
- [20] X. Li, J. Li, W. Liu, Y. Zhang, and H. Shan, "Group sparse based joint power and resource block allocation design of hybrid Device-to-Device and LTE-advanced Networks," *IEEE Journal on Selected Areas in Communications*, vol. 34, no. 1, pp. 41–57, January 2016.
- [21] H. A. Mustafa, M. Z. Shakir, M. A. Imran, A. Imran, and R. Tafazolli, "Coverage gain and Device-to-Device user density: stochastic geometry modeling and analysis," *IEEE Communications Letters*, vol. 19, no. 10, pp. 1742–1745, October 2015.
- [22] N. Lee, X. Lin, J. G. Andrews, and R. W. Heath, "Power control for D2D underlaid cellular networks: modeling, algorithms, and analysis," *IEEE Journal on Selected Areas in Communications*, vol. 33, no. 1, pp. 1–13, January 2015.
- [23] J. Andrews, F. Baccelli, and R. Ganti, "A tractable approach to coverage and rate in cellular networks," *IEEE Transactions on Communications*, vol. 59, no. 11, pp. 3122–3134, November 2011.
- [24] 3GPP TSG-RAN WG1-76BIS, R1-141820, "Simulation assumptions for impact of D2D on WAN," April 2014.
- [25] 3GPP TSG-RAN WG1-74, R1-133600, "Techniques for D2D discovery," August 2013.
- [26] P. S. Segundo, "A new DSATUR-based algorithm for exact vertex coloring," *Computers and Operations Research*, vol. 39, no. 7, pp. 1724–1733, July 2012.
- [27] I. Gradshteyn, and I. Ryzhik, "Table of integrals, series, and products," in *IEEE 80th Vehicular Technology Conference (VTC Fall)*, San Diego, USA, 2007.